

General Disclaimer

One or more of the Following Statements may affect this Document

- This document has been reproduced from the best copy furnished by the organizational source. It is being released in the interest of making available as much information as possible.
- This document may contain data, which exceeds the sheet parameters. It was furnished in this condition by the organizational source and is the best copy available.
- This document may contain tone-on-tone or color graphs, charts and/or pictures, which have been reproduced in black and white.
- This document is paginated as submitted by the original source.
- Portions of this document are not fully legible due to the historical nature of some of the material. However, it is the best reproduction available from the original submission.

CHEMICAL VAPOR DEPOSITION GROWTH

QUARTERLY REPORT NO. 1

(NASA-CR-148319) CHEMICAL VAPOR DEPOSITION
GROWTH Quarterly Report (Rockwell
International Corp., Anaheim, Calif.) 76 p
HC \$5.00 C SCL 07D

N76-27384

Unclas
42370

G3/25

Contract No. 954372

"This work was performed for the Jet Propulsion Laboratory,
California Institute of Technology, under NASA Contract NAS7-100
for the U. S. Energy Research and Development Administration,
Division of Solar Energy.

The JPL Low-Cost Silicon Solar Array Project is funded by ERDA
and forms part of the ERDA Photovoltaic Conversion Program to
initiate a major effort toward the development of low-cost solar arrays."



Rockwell International



CHEMICAL VAPOR DEPOSITION GROWTH

QUARTERLY REPORT NO. 1

31 March 1976

By

R. P. Ruth, H. M. Manasevit, J. L. Kenty,
L. A. Moudy, W. i. Simpson and J. J. Yang

Contract No. 954372

"This work was performed for the Jet Propulsion Laboratory,
California Institute of Technology, under NASA Contract NAS7-100
for the U. S. Energy Research and Development Administration,
Division of Solar Energy.

The JPL Low-Cost Silicon Solar Array Project is funded by ERDA
and forms part of the ERDA Photovoltaic Conversion Program to
initiate a major effort toward the development of low-cost solar arrays."

ROCKWELL INTERNATIONAL
Electronic Research Division
Anaheim, CA 92803

ABSTRACT

The activities of the first quarter of the contract, which began December 29, 1975, are described. An existing laboratory-type CVD reactor system with a vertical deposition chamber has been used for growth of the Si films studied to date. Extensive modifications of this system, involving mass flow controllers and automatic timing of reactant gas flows by means of solenoid-activated air-operated bellows valves, will be completed early in the second quarter.

Several potential suppliers of candidate substrate materials have been contacted. Numerous samples of materials have been received for consideration, some of which have been evaluated experimentally as substrates for CVD of Si by pyrolysis of SiH_4 in H_2 or He carrier gases. Materials of three main classes - glasses, glass-ceramics, and polycrystalline ceramics - are being investigated.

Preliminary deposition experiments with two of the available glasses have not been encouraging because of adverse physical and/or chemical effects on the glass in the CVD process, even at relatively low temperatures. Moderately encouraging results, however, have been obtained with fired polycrystalline alumina substrates, which have been used for Si deposition at temperatures above 1000°C . These materials exhibit some preferred orientation in their polycrystalline structures, and the films grown on these are also preferentially oriented, although no crystallographic correlations have yet been made.

The surfaces of both the substrates and the films have been characterized by x-ray diffraction, reflection electron diffraction, scanning electron microscope, optical microscopy, and surface profilometric techniques. Some evidence of improved surface grain size has been found in some aluminas subjected to high-temperature firing cycles beyond those normally used, and the polishing of some alumina wafers to produce better surfaces for Si film deposition and grain growth has begun.

A variety of CVD experiments has been carried out to establish baseline performance data for the reactor system, including temperature distributions on the sample pedestal, effects of carrier gas flow rate on temperature, effects of carrier gas flow rate on film thickness uniformity in H_2 and in He (with H_2 producing more uniform results), and Si film growth rate by SiH_4 pyrolysis as a function of temperature for H_2 and for He. An activation energy for the deposition process in the temperature range up to $850\text{--}900^\circ\text{C}$ of ~ 1.8 eV was found for either carrier gas. Above that temperature range the growth rate still increases with temperature in H_2 but with a much lower activation energy (~ 0.14 eV). For He the rate passes through a maximum at $850\text{--}900^\circ\text{C}$, decreasing rapidly for further increases in temperature, indicating a difference in the deposition process at high temperatures ($>850^\circ\text{C}$) in the two gases. Generally, better looking Si films have been achieved to date by deposition in H_2 than in He.

X-ray diffraction methods have been used to obtain preliminary information on the amount of preferred orientation and the grain size in CVD Si films deposited on polycrystalline alumina at several different temperatures. Methods of SEM analysis and classical metallography combined with etching procedures have been used to provide evidence of vertical or columnar growth in some of the Si films on alumina. Only limited electrical measurements have been made, primarily because of the emphasis on structural properties of the films to date and the fact that only undoped films have been prepared; experiments with doped films will be initiated early in the second quarter.

Several samples have been sent to OCLI for experimental processing into solar cell structures. Preliminary results obtained on the first group of four to be processed were not encouraging. The films were thin and undoped, and considerable difficulty was encountered in processing them by standard solar cell fabrication techniques.

Conclusions and recommendations based on the first quarter of work are outlined, and specific plans for the next quarter are given. Manpower and funding expenditures are summarized, and the updated technical program plan is given.

CONTENTS

	<u>Page</u>
1. Introduction	1
2. Technical Discussion	3
2.1 Task 1. Modification and Test of Existing CVD Reactor System	3
2.2 Task 2. Identification/Development of Suitable Substrate Materials	7
2.3 Task 3. Experimental Investigation of Si CVD Process Parameters	24
2.4 Task 4. Preparation of Si Sheet Samples	47
2.5 Task 5. Evaluation of Si Sheet Material Properties	47
2.6 Task 6. Fabrication and Evaluation of Solar Cell Structures	58
3. Conclusions and Recommendations	63
4. Plans for the Next Quarter	65
5. New Technology	69
6. References	71
Appendix A. Manpower and Funding Expenditures	73
Appendix B. Updated Technical Program Plan	75

PRECEDING PAGE BLANK NOT FILMED

ILLUSTRATIONS

<u>Figure</u>	<u>Page</u>
2-1. Schematic Diagram of Vertical-Chamber Chemical Vapor Deposition Apparatus for Si Sheet Growth	4
2-2. Schematic Diagram of Si CVD Reactor System Incorporating Planned Modifications	6
2-3. Linear Thermal Expansion Coefficients as a Function of Temperature	10
2-4. Evidence of Contamination of CVD Si Film Growth on Sapphire	14
2-5. Edge View Showing Bowing of Composite of CVD Si on Code 7059 Glass	15
2-6. Nonuniformity in ASM701 (Corierite) Substrate Revealed by Si CVD Film Growth	15
2-7. Nonuniformities in Large-Grain Alumina "Tape Product" (Coors), Emphasized by Si CVD Growth	16
2-8. Wrinkled CVD Si Film Grown 14 μm Thick on Glazed Alumina Substrate	17
2-9. Surface Morphology of ASM805 Fired Alumina Substrate	19
2-10. Surface Morphology of Fired Alumina Substrates	20
2-11. Surface Morphology of ASM805 Alumina Substrate Refired	21
2-12. Surfaces of 4 Vistal (Coors) Polycrystalline Alumina Substrates after Successive Firings	23
2-13. Schematic Diagram of Apparatus Arrangement for Measuring Pedestal Temperature with Infrared Radiation Thermometer ($2.0 \leq \lambda \leq 2.6 \mu\text{m}$)	25
2-14. Observed Temperature Difference ($T_t - T_c$) on Top of rf-Heated Pedestal for H_2 and He Carrier Gases at Three Different Flow Rates	28
2-15. Si Film Deposition on (01 $\bar{1}2$) Sapphire Substrates as Function of Reciprocal Temperature for SiH_4 Pyrolysis in H_2 and in He	33
2-16. Bubbles Formed at Interface of CVD Si Film Grown on Corning Code 1723 Glass Substrate at $\sim 650^\circ\text{C}$ in He	35
2-17. Rosette Surface Structures of CVD Si Films Grown on Fired Polycrystalline Alumina Substrates in H_2 at 1025°C by SiH_4 Pyrolysis	38
2-18. High Magnification Views of Rosette Surface Structures on CVD Si Films	39
2-19. Rosette Surface Structures on CVD Si Films Grown on ASM805 Substrates in H_2 at $\sim 1025^\circ\text{C}$	41
2-20. SEM Photographs of Cleaved Cross Sections of CVD Si Films Grown on ASM805 Substrates	42
2-21. Appearance of Cleaved Cross Section of 40- μm -thick CVD Si Film	43
2-22. Metallic Cross Section of 40- μm -thick CVD Si Film	44
2-23. Composite Photomicrograph Showing Detail of Central Region of Figure 2-22	45
2-24. SEM Photographs of Metallographic Cross Section of Figures 2-22 and 2-23	46

ILLUSTRATIONS (Cont)

<u>Figure</u>		<u>Page</u>
2-25.	Dektak Profilometer Traces for As-Fired Surfaces of Polycrystalline Alumina Substrates and for As-Grown Surfaces of CVD Si Films	50
2-26.	Dektak Profilometer Traces of Surfaces of Vistal (Coors) Polycrystalline Alumina Substrates Subjected to Four Different Firing Histories	51
2-27.	Hall-Effect Bridge Pattern Photolithographically Etched in CVD Si Film	56
2-28.	Schematic Diagram of Apparatus for MOS Capacitance-Voltage Measurements	57

TABLES

<u>Table</u>	<u>Page</u>
2-1. Possible Glasses for Si Growth Studies*	9
2-2. Candidate Substrate Materials Received to Date from Various Suppliers	13
2-3. Representative Properties of Polycrystalline Alumina Ceramics from Three Manufacturers	18
2-4. Apparent Surface Grain Size of Several Polycrystalline Alumina Substrates as Measured in SEM	22
2-5. Observed Temperature Settings at Three Locations on SiC-Coated Carbon Pedestal (100 dia) for H ₂ and He Carrier Gases	26
2-6. Si Film Thickness Uniformity Obtained with He as Carrier Gas (Single-Crystal (0112) Al ₂ O ₃ Substrates)	29
2-7. Si Film Thickness Uniformity Obtained with H ₂ as Carrier Gas (Single-Crystal (0112) Al ₂ O ₃ Substrates)	31
2-8. CVD Si Growth Rate Data for Pyrolysis of SiH ₄ in H ₂ Using (0112) Sapphire Substrates*	32
2-9. CVD Si Growth Rate Data for Pyrolysis of SiH ₄ in He Using (0112) Sapphire Substrates*	32
2-10. Average Measured Surface Roughness of Polycrystalline Alumina Substrates Measured by Surface Profilometry with Sloan Dektak	48
2-11. CVD Si Sheet Samples* Submitted to OCLI for Solar Cell Processing and Measurement.	59

1. INTRODUCTION

This contract began December 29, 1975, and is of 18-month duration. This first quarterly report covers nominally the first three months of the program. However, because of the holiday shutdown at the beginning of this period and the fact that the report must be prepared prior to the end of the calendar quarter, less than a full three months of work is described.

The purpose of the contract is to explore the chemical vapor deposition (CVD) method for the growth of Si sheet on inexpensive substrate materials. The work is carried out at the Rockwell Electronics Research Division in Anaheim, but also involves experimental solar cell fabrication and evaluation by the Photoelectronics Group of Optical Coating Laboratory, Inc. (OCLI), in City of Industry, California.

The formal objective of the contract is development of CVD techniques for producing large areas of Si sheet on inexpensive substrate materials, with sheet properties suitable for fabricating solar cells meeting the technical goals of the Low Cost Silicon Solar Array Project (LCSSAP). The techniques developed are to be directed toward minimum-cost processing, production of sheet having properties adequate to result in cells with terrestrial array efficiency of 10 percent or more, and eventual scale-up to large-quantity production.

The CVD method as applied to Si sheet growth involves pyrolysis or reduction of a suitable Si compound at elevated temperature and approximately atmospheric pressure in a flow-through (open-tube) system. A carrier gas is used to transport the reactants to the deposition chamber in which the substrate is mounted on a SiC-coated carbon pedestal heated by rf from outside the chamber. The properties of the Si sheet are determined by deposition temperature, reactant concentrations, the nature of the carrier gas, the Si source compound used, growth rate, doping impurities (added by introduction of appropriate compounds into the carrier gas stream), and the properties of the substrate.

The specific technical goals established for the contract include the following:

Si sheet area (per sample)	30 cm ²
Si sheet deposition rate	5 μm per min
Si sheet thickness	20 to 100 μm
Si sheet crystal structure	100 μm average grain size
Intragrain dislocation density	<10 ⁴ per cm ²

The principal technical problems to be solved in the program are (1) establishing preferred CVD process parameters (temperature, reactant concentrations, carrier gas composition, doping impurities, growth rate) for optimized intragrain properties for the Si sheet grown on various substrate materials, (2) identifying suitable substrate materials that will survive the environment of the CVD process and be potentially inexpensive and available in large areas, yet be as favorable as possible to Si grain growth, and (3) achieving adequate grain size in the Si sheet to provide satisfactory solar cell properties.

Si sheet growth by CVD on inexpensive substrates will quite likely be polycrystalline, because such substrates will be either amorphous or microcrystalline and will thus provide little or no ordering influence on the growth mechanism. This is, of course, contrary to the case of epitaxial growth of Si on single-crystal substrates.

However, many characteristics of the CVD method indicate that it has considerable promise for achieving the 1985 technical and cost goals of the LCSSAP: (1) it produces only that amount of Si that is actually required for the photovoltaic effect, without the requirement of additional Si for purely structural reasons; (2) it is a relatively low-temperature process and thus is energy-conservative; not requiring melting of Si at any stage; (3) it does not require refined/purified polycrystalline Si starting material, using instead a high-purity compound of Si that is actually a product of one of the early steps in the preparation of polycrystalline semiconductor-grade Si; (4) it is inherently a large-area process, capable of potential scale-up to areas that are practical for large array fabrication in the LCSSAP; (5) impurity doping for junction formation can be carried out during CVD growth of the Si sheet; (6) thicknesses are closely controllable by valve and flowmeter adjustments; and (7) it has the capability for eventual development of a continuous fabrication process, in which the Si material, the junction or barrier, and the required contacts are all fabricated in a single integrated series of operations in one apparatus.

Thus, although it may be found difficult to achieve the project goal of 10 percent terrestrial array efficiency in polycrystalline Si sheet solar cells, the prospects of at least closely approaching that are considered good. The chances of realizing sufficient cost reduction per unit area of active cell surface appear strong enough that a cost-per-watt figure within the project goals should be achievable with this process.

The contract program is structured in terms of six main technical tasks, as follows: (1) modification and test of an existing CVD reactor system; (2) identification and/or development of suitable inexpensive substrate materials; (3) experimental investigation of CVD process parameters using various candidate substrate materials; (4) preparation of Si sheet samples for various special studies, including solar cell fabrication; (5) evaluation of the properties of the Si sheet material produced by the CVD process; and (6) fabrication and evaluation of experimental solar cell structures by OCLI, using standard and near-standard processing techniques.

The progress achieved to date in the contract is described by task in the following section, followed by a summary of conclusions and recommendations and an outline of the work planned for the second quarter. This is followed by the New Technology statement and a listing of the references for the technical discussion.

The manpower and funding expenditures are summarized in Appendix A, and the Updated Technical Program Plan is included as Appendix B.

2. TECHNICAL DISCUSSION

This section contains a discussion of the results obtained to date in performance of the Statement of Work of this contract, including a summary of the characterization data developed during the first quarter and interpretation of the results where appropriate. This discussion is arranged by task, in general, although the interlocking of the tasks is such that this distinction is not always possible.

2.1 TASK 1. MODIFICATION AND TEST OF EXISTING CVD REACTOR SYSTEM

The apparatus required for the chemical vapor deposition of Si films is relatively simple and has been highly developed in recent years. It consists of six main components: (1) deposition chamber (reactor), with provision for supporting the heated substrates on which Si deposited; (2) reactant gas manifold and distribution line system, with appropriate metering, valving, and controls; (3) reservoirs or tanks of the required reactant and carrier gases, with associated purifiers and/or filters; (4) vacuum system for evacuating selected portions of the reactor and gas manifold, as needed; (5) provision for burning, reprocessing, or otherwise discharging the exhaust gases exiting from the reactor system; and (6) power supply for heating the substrates in the reactor chamber - usually an rf generator with an external coil which couples to a susceptor, which also serves as the substrate support.

In the early stages of this program an existing laboratory-type CVD reactor system with a vertical deposition chamber has been used. This system is similar to that used extensively at Rockwell in previous studies of semiconductor epitaxial growth by CVD and is described in detail elsewhere (Ref 1). It is shown schematically in simplified form in Figure 2-1.

Even in its simplest form a system of this type provides at least the following important capabilities:

1. Growth of undoped or doped Si films on any substrate that will withstand the growth temperature, using several different sources of Si, including SiH_4 or a Si halide or mixtures of SiH_4 and HCl
2. Etching of Si on the substrate or removing solid reaction products from the walls between deposition experiments, using HCl
3. Use of one or more carrier gases to establish a desired growth atmosphere
4. Evacuation of sections of the apparatus, including the reactor, while gas flows are continued in other sections
5. "Homogenization" of gas flows prior to introduction of the gases into the reactor
6. Trapping of moisture and other condensables that are not representative of the carrier gases, reactants, and dopants used but instead are probably typical of the impurities present in "electronic grade" gases.

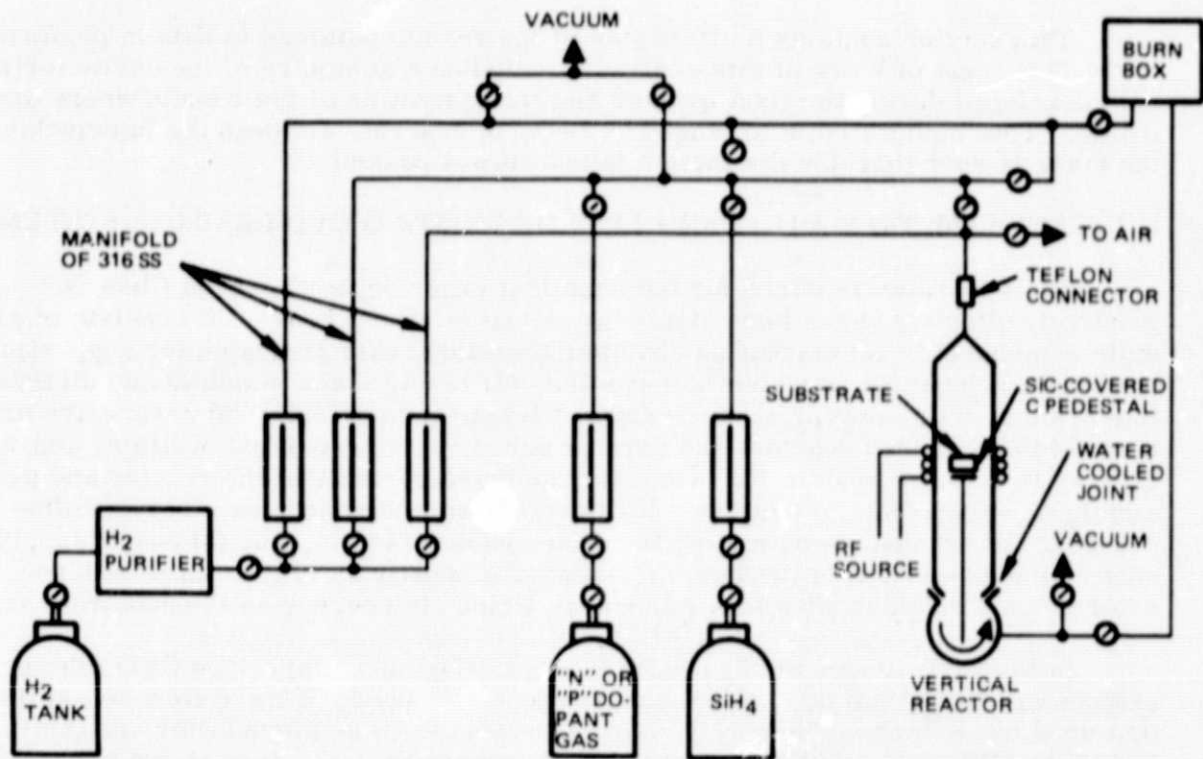


Figure 2-1. Schematic Diagram of Vertical-Chamber Chemical Vapor Deposition Apparatus for Si Sheet Growth

To improve the control of the Si CVD process to be used in this program a number of modifications are scheduled to be made in the reactor system shown in Figure 2-1. The design details of these modifications were finalized during the first month, as planned. This resulted in some additions being included beyond those considered prior to start of the contract. These additional changes will lead to a more versatile system offering greater reproducibility and reliability than that initially suggested.

All parts and components necessary for these modifications have now been received, with the exception of two printing recorders. However, because of delayed delivery of some of the key items by vendors it has been necessary to reschedule the completion of the reactor system modifications to April.

It is now planned that 13 Tylan Model FC-260 Mass Flow Controllers will be installed on the reactor system. All gas lines involved directly in the CVD process will be controlled by this means. The only lines not so controlled will be the carrier gas bypass and reactant "dump-out" line leading to the burn-box at the top of the reactor-system hood enclosure and a separate H₂ line to admit that gas to the chamber for pre-deposition "etching" when carrier gases other than H₂ are being used.

The 13 controllers to be installed are as follows:

- 2 in parallel main gas flow lines, one leading into the reactor chamber and the other provided for mixing reactants in desired proportions and to constant total flow prior to introduction into the chamber
- 3 in Si source compound supply lines (SiH_4 , SiH_2Cl_2 , and a bubbler for SiHCl_3 and SiCl_4)
- 1 in bubbler-source carrier gas line
- 1 in HCl line
- 2 in dopant lines (n- and p-type impurity source compounds)
- 2 in gas lines for dilution of doping compounds
- 2 in diluted dopant lines (n and p type)

A Tylan Model GPT-104 Automatic Sequence Timer will be associated with these controllers; it is capable of providing automatically-timed control of flow intervals in 10 different lines (i. e., 10 signal channels), with up to four different events (such as on and off) per channel programmable in each cycle of the sequencer.

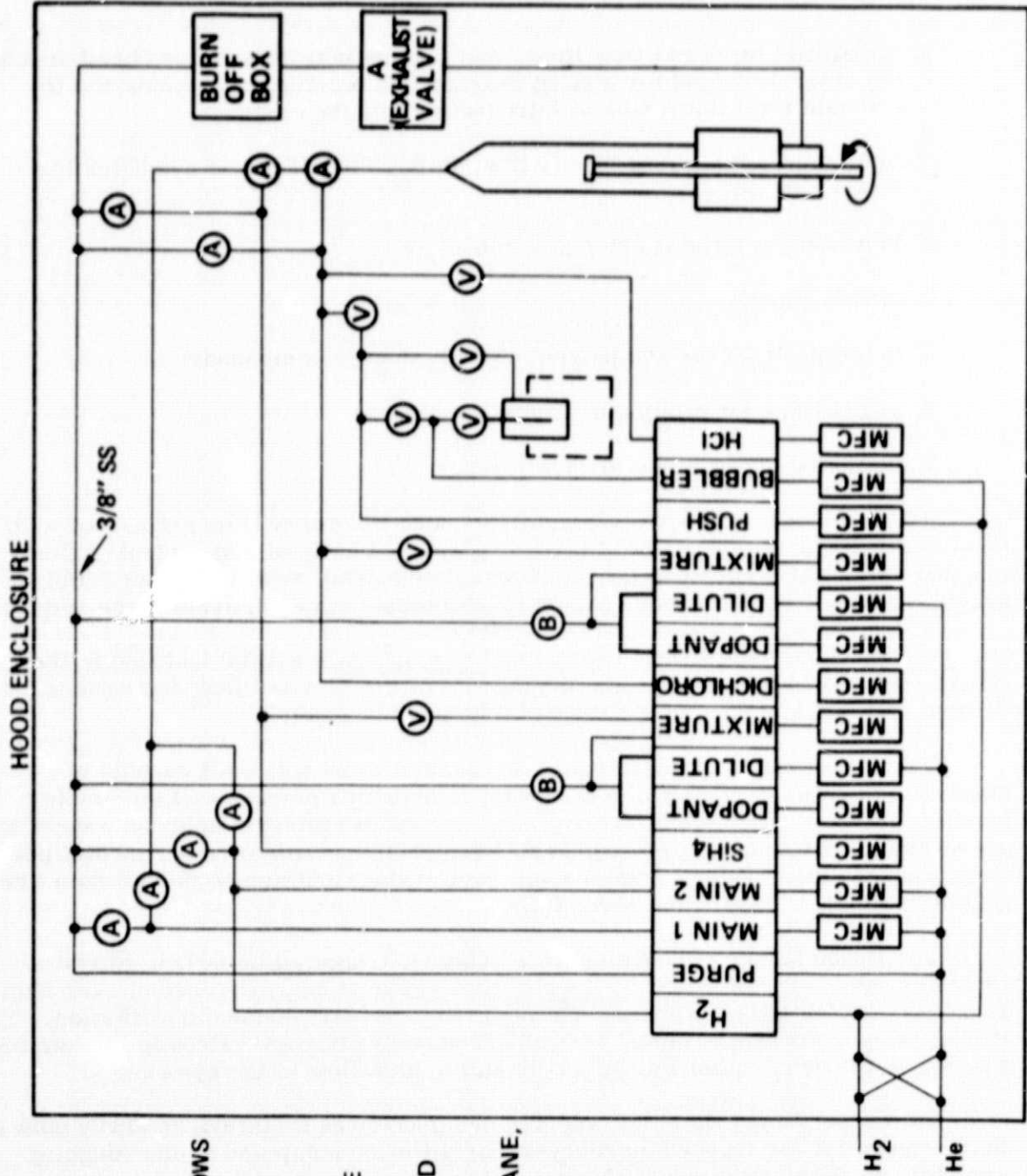
Four Tylan Model RO-14 control and readout units will be included in the centralized control panel to handle the outputs of the 13 mass flow controllers. Each readout unit has a maximum capacity of four input channels.

Two Model 5150A Hewlett-Packard Thermal Printers, each capable of sequential printing of 20 channels of digital information per cycle of the printer (printing time $\sim 1/3$ sec per line, data input acceptance interval adjustable down to one second), will also be used to provide permanent records of experimental parameters when desired. These printers will each include a timer so that all data are related to printed digital time recordings.

Ten Nupro Model 4BK air-operated valves, triggered by switch-activated solenoids, are being installed on the reactor system to improve control over film thickness, nucleation phenomena, and impurity concentration and distribution. Two of these valves are Nupro Model SS-4BK-S2 zero-dead-space valves to further reduce the amount of uncontrolled and/or unwanted reactant flow in the system.

An Alcatel Model ZM2012C vacuum pump has been installed, to serve both as the forepump for the trapped mercury-vapor diffusion pump and as the roughing pump for the reactor system. This type of pump has improved pumping speed over conventional oil-immersed mechanical vane pumps, provides essentially zero back-streaming of hydrocarbon vapors because of its "dry" construction, and is relatively quiet in operation.

A schematic diagram of the Si CVD reactor system incorporating the planned modifications is shown in Figure 2-2. Although additional changes may be made at the time of final reassembly of the system, this is the configuration now believed to meet the requirements of the anticipated contract work.



- NOTES:**
- ALL TUBING ONE-QUARTER IN. SS EXCEPT AS NOTED
 - V = MANUAL BELLOWS VALVE
 - A = AIR OPERATED BELLOWS VALVE
 - B = BACK-PRESSURE REGULATOR
 - ALL GASES TRAPPED WITH COLD TRAPS
 - SiH₄, DICHLOROSILANE, N AND P DOPANTS, AND HCl PIPED IN FROM SEPARATE FUME HOOD TO APPROPRIATE MFC
 - MFC = MASS FLOW CONTROLLER

Figure 2-2. Schematic Diagram of Si CVD Reactor System Incorporating Planned Modifications

In addition to the reactor system itself, which is enclosed in a separate high-flow-rate fume hood, an external control center will be housed in a separate floor-mounted cabinet at the side of the hood. This cabinet will accommodate the sequence timer, the four readout units, two recorder-printers, and the master valve control panel. This unit is not indicated in the diagram of Figure 2-2.

Until the modifications are completed early in the next quarter the CVD experiments will continue to be done in the existing system. All results reported herein involve the use of the existing reactor, with only minor modifications having been made since the start of the contract work.

2.2 TASK 2. IDENTIFICATION/DEVELOPMENT OF SUITABLE SUBSTRATE MATERIALS

The 1985 cost goals of the LCSSAP are such that it now seems almost entirely out of the question that any single-crystal substrate material (other than perhaps Si itself) could be used for the purpose. Future developments, of course, could conceivably alter this outlook, but for the requirements of this contract it appears that other materials far less favorable to Si crystal growth must be considered and evaluated.

With that as a starting premise the search for candidate substrate materials was begun. These efforts have produced some materials for consideration, as described below.

2.2.1 Rationale for Material Selection

In attempting to identify candidate substrate materials for CVD growth of Si sheet which will meet the technical goals of this contract, discussed in the Introduction, several considerations are necessary. First of all, the material must be potentially inexpensive. This means that, as an absolute upper limit in today's market as well as in 1985, it must be less expensive than Si itself for comparable sizes and shapes. More will be said on the subject of present and projected costs of candidate substrate materials in later reports.

Next, it must be available, or potentially so, in relatively large areas. Present technology probably should already have produced similar material in sizes larger than commercially available Si.

In addition, the properties of the substrate material should be compatible with those of Si. Its linear thermal expansion behavior should parallel that of Si as closely as possible from at least the Si sheet deposition temperature down to room temperature. The Si film must also be chemically stable with respect to the substrate surface, so that the transition layer at the interface does not cause separation of the two components. Also, the substrate surface must be stable relative to the carrier gas and the products of Si formation, notably H_2 when SiH_4 is the source of Si and HCl when the Si-containing halides are used to produce the Si.

Only a few classes of materials now commercially available could be considered initially as candidate substrate materials, based on cost, availability, and reported properties. These include the amorphous glasses, glass-ceramics, and polycrystalline ceramics. Many glasses are available in very large sheet form, and others are

potentially susceptible to fabrication into sheets. Some glass-ceramics are also produced in large sheets (the order of square meters), and many of the polycrystalline ceramic materials are available in areas up to about 300 cm².

In contemplating the use of an amorphous glass as a substrate, it is necessary to consider the effect of temperature on certain glass properties, notably the thermal expansion coefficient and the viscosity. Convention has assigned certain viscosity values to some of the physical characteristics that are important to the application of interest in this program:

Strain point $\sim 3 \times 10^{14}$ poises

Annealing point $\sim 10^{13}$ poises

Softening point $\sim 10^{7.6}$ poises

Working point $\sim 10^4$ poises

From room temperature to just below the strain point, which is generally regarded as the upper limit for use of an annealed glass, thermal expansion coefficients (TEC) for glasses tend to remain nearly constant, increasing only slightly with temperature. However, with further increase in temperature into the annealing range the viscosity decreases and a large and rapid increase in TEC occurs. Although the reduction in viscosity at temperatures above the annealing point might seem to eliminate a glass from consideration for possible use as a substrate for Si sheet growth in that temperature range, there have been studies of Si layer growth on such surfaces in the past (Ref 2), and such a system might again warrant investigation.

Some representative glasses commercially available from Corning Glass Works, and in some instances from Owens-Illinois and other glass manufacturers, are listed in Table 2-1. Most of the glasses in the table have TEC values between those of Si and sapphire (α -Al₂O₃) for the range 25°C to the setting point, although that is not accurately indicative of the TEC values at higher temperatures.

This is shown more clearly by the curves of Figure 2-3, which gives TEC data for Si and several possible substrate materials of interest, including glasses, throughout the range from room temperature up to Si CVD deposition temperatures. Further reference will be made to these data in later discussions.

Although many of the glasses listed in Table 2-1 are not normally available in plate or flat-substrate form, it is considered that flat substrates could be produced by techniques well-known in the glass industry.

Among the glasses presented in the table, only two have strain points above the lowest temperatures at which Si growth is considered technically possible by CVD techniques; these are the aluminosilicates Code 1720 and Code 1723. However, as noted above, Si growth by CVD on the other examples could be possible at temperatures between the annealing point of the glass and its softening point, i. e., above $\sim 600^\circ\text{C}$, which is the lowest temperature consistent with growth of Si from SiH₄.

Table 2-1. Possible Glasses for Si Growth Studies*

Corning Glass Code	Type of Glass	Forms Usually Available**	Thermal Expansion Coefficient Multiply by 10 ⁻⁷ /°C (25°C to Setting Point ***)	Viscosity Data			
				Strain Point (°C)	Annealing Point (°C)	Softening Point (°C)	Working Point (°C)
0317	Alumina Soda Lime	S	87 (0-300°C)	574	622	871	-
1720	Aluminosilicate	BT	52	667	712	915	1202
1723	Aluminosilicate	BT	54	665	710	908	1168
2405	Borosilicate	BTU	53	501	537	765	1083
3320	Borosilicate	-	43	493	540	780	1171
7040	Borosilicate	BT	54	449	490	702	1080
7050	Borosilicate	T	51	461	501	703	1027
7052	Borosilicate	BMPT	53	436	480	712	1128
7056	Borosilicate	BTP	56	472	512	718	1058
7059†	Borosilicate	S	46 (0-300°C)	587	635	842	1160
7070	Borosilicate	BMPT	39	456	496	-	1068
7251	Borosilicate	P	38.1	500	544	780	1167
7720	Borosilicate	BPT	43	484	523	755	1146
7740	Borosilicate	BPSTU	35	510	560	821	1252
7760	Borosilicate	BP	37	478	523	780	1198
9741	Borosilicate	BUT	50	408	450	705	1116.

* From "Properties of Glasses and Glass-Ceramics," Corning Glass Works

** B - Blown ware; M - Multiform; U - Panels; P - Pressed ware; S - Plate glass; T - Tubing and rod

*** Setting point is defined as 5°C above strain point

† From Corning Product Information Sheets or private communication

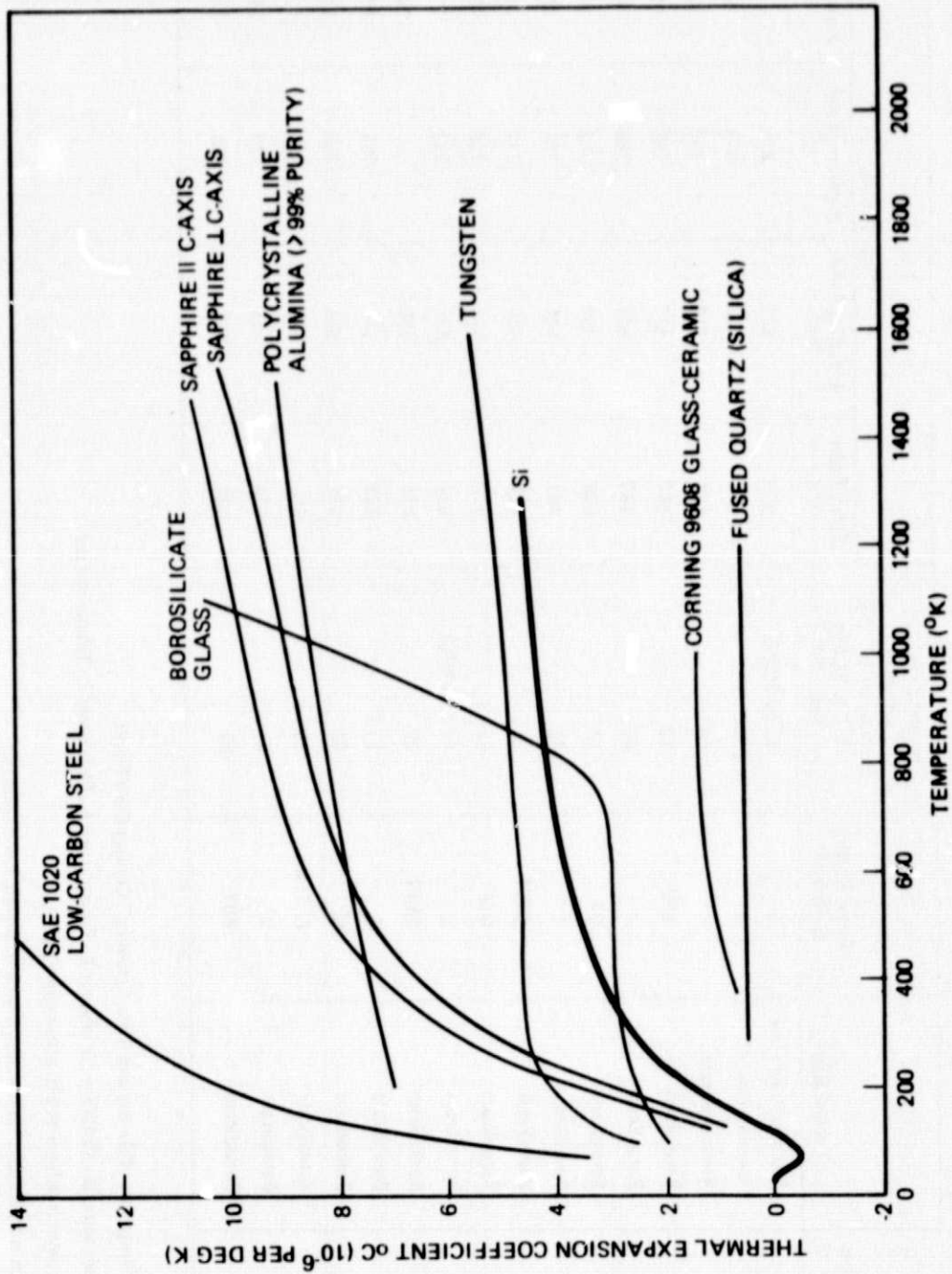


Figure 2-3. Linear Thermal Expansion Coefficients as a Function of Temperature for Si and Several Possible Substrate Materials

Since it has not yet been determined with certainty in what condition of viscosity a glass surface should be for the best formation of Si films of solar-cell quality, glasses should not be ruled out of consideration at this time. However, since studies of polycrystalline growth of Si on SiO₂ indicate that higher temperatures lead to increased grain size (Ref 3), early evaluation of glasses should involve those glasses which possess at least relatively high softening points.

Glass-ceramics are materials which have been converted from their original glassy state to polycrystalline ceramics by controlled nucleation and devitrification. Through variations in composition and heat treatment, glass-ceramics offer a wide range of grain size, crystallite orientations, and thermal expansion coefficients, from high positive values to negative values, including some that are zero over a limited temperature range. It is anticipated that during this program glass-ceramics with TEC's similar to that of Si will be obtained and evaluated as substrates for solar cell structures.

The third class of substrate material of initial interest is the polycrystalline ceramic, which is available in many compositions and purities. Based on TEC values only (cf Figure 2-3), likely materials for study include zircon (ZrO₂ · SiO₂), with TEC ~4.9x10⁻⁶ per deg C (25-900°C); cordierite (2MgO · 2Al₂O₃ · 5SiO₂), with TEC ~3.7x10⁻⁶ per deg C (25-900°C); a number of aluminas, with TEC's 7.7-8.0x10⁻⁶ per deg C (25-900°C), and mullite (3Al₂O₃ · 2SiO₂), with TEC ~4.8x10⁻⁶ per deg C (40-800°C). In today's market, demand has produced "supersmooth" as-fired surfaces only on the aluminas. Further studies in producing better surfaces (without polishing) on the other ceramics are necessary and are in progress in the laboratories of some of the manufacturers.

Another type of substrate material for consideration as a substrate for Si sheet growth is a combination of two of the above classes, namely, a glass film produced upon a polycrystalline ceramic, i. e., a glazed ceramic. The typical glaze formed on a ceramic offers a surface finish better than that which can be achieved on the ceramic itself (in an as-fired condition) without polishing. The glaze fills in the pores of the surface and can be used with a relatively inexpensive non-smooth substrate of purity lower than, for example, 99.5 percent Al₂O₃. Presently, however, the commercial availability of glazed ceramics is very limited, and glazes with low softening temperatures appear to be the rule. This type of composite is attractive, however, and various glazes will probably be evaluated in this program. The possibility of utilizing other types of composite substrate will also be evaluated as the work progresses.

2.2.2 Contacts with Potential Substrate Suppliers

Prior to the start of this contract, telephone contacts were made with four potential suppliers of substrates for this program; 3M Company, Corning Glass Works, Coors Porcelain Company, and Owens-Illinois, Inc. Their initial responses led to receipt of samples of a number of commercially available and research-type candidate materials; from 3M Company, Laurens, SC --ASM701 (cordierite), ASM475 (zircon), ASM743 (a glazed Al₂O₃), ASM805 (sintered Al₂O₃); from Corning Glass Works, Corning, NY--Codes 1723, 0221, 7059, and 0317 glasses; from Coors Porcelain Company, Golden, CO--large-grained Al₂O₃; and from Owens-Illinois, Inc., Toledo, OH--a special high-temperature glass.

Samples of most of the above substrates were used early in the contract program in exploratory Si CVD experiments using SiH_4 as the source of Si and either H_2 or He as the carrier gas. These experiments were designed to prepare composites for use in discussions during a visit to these and other potential substrate suppliers during the first month of the program.

A contract-sponsored trip to seven different potential suppliers was completed early in the quarter. In addition to the above-listed companies, visits were made to Materials Research Corporation (MRC), Orangeburg, NY; W. R. Grace and Co., Columbia, MD; and Pemco-Glidden-Durkee, Baltimore, MD.

Subsequent to that trip, new discussions were held with Chicago Vitreous Corporation, Cicero, IL, a manufacturer of glazes for metals; Atomics International, a division of Rockwell, developer of a high-temperature glass deposited on various metal components for use in nuclear reactor applications; Kyocera, a ceramic manufacturer based in Japan; Magneco, a small-business ceramic manufacturer in Addison, IL; and Union Carbide Corporation, Carbon Division, Parma, OH, producer of highly-oriented crystalline carbon substrates.

Several of these manufacturers have indicated a strong interest in attempting to prepare and supply samples of non-standard glasses, glass-ceramics, ceramics, and glazes for exploratory use in this program. Some indicated the effort could probably not continue throughout the contract period without some specific financial support, from the contract or otherwise. Only W. R. Grace and Co. and Magneco will not be supplying experimental samples of substrate materials for evaluation during the early phases of this program.

Four of the other suppliers of substrate materials - Corning, 3M, Kyocera, and MRC - visited the Rockwell Electronics Research Division during February to discuss details of the substrate requirements. Specially prepared samples of Corning Code 1723 glass were delivered by the Corning personnel at that time, for experimental use on the contract.

Table 2-2 lists all of the substrate materials samples of which have been received from various vendors to date. Approximately half of the materials listed were received during the month of March. Results of characterization of many of these will be reported in the next quarterly report.

2.2.3 Preliminary Evaluation of Candidate Materials

Before a potential new substrate material is used for Si growth, the following characteristics, determined on representative samples, are established: physical appearance (unaided eye); thickness; surface roughness; general appearance at 100X and/or 450X magnification; and (optional) structural properties determined by such procedures as x-ray, reflection electron diffraction (RED), and SEM examination of the surface, when advisable.

Substrates of interest are then subjected to exploratory Si CVD growth in both H_2 and He atmospheres at temperatures consistent with the reported properties of the material. For example, for free-standing glasses temperatures below the softening point are used; for glazes on ceramics, higher than softening temperatures

Table 2-2. Candidate Substrate Materials Received to Date from Various Suppliers

SUBSTRATE IDENTIFICATION	MATERIAL/TYPE	THERMAL EXPANSION COEFF. (TEMP RANGE) (10 ⁻⁶ PER DEG C)	SURFACE ROUGHNESS OR FINISH	THICKNESS (INCHES)	NOMINAL PURITY (%)
Corning 0221* 0317* 1723* 7059*	Lime Borosilicate	7.4 (0-300°C)	< 0.5 Microinch	0.010	-
	Alumina Soda Lime	8.7 (0-300°C)		0.060	-
	Aluminosilicate	5.4 (25-670°C)		0.030, 0.050	-
	Barium Alumino-borosilicate	4.6 (0-300°C)		0.032	-
Owens-Illinois* GS-186	Proprietary High-temperature Glass	4.7 (0-300°C)	Mechanically Polished: Prob < 1 Microinch	0.030, 0.040	-
	"	3.8 (0-300°C)		0.040	-
	"	3.6 (0-300°C)		0.040	-
Coors ADS 96F ADS 995 Refired Large-grain Al ₂ O ₃ * Vistal	"	2.6 (0-300°C)	As Fired	0.042	-
	Alumina	8.1 (25-1000°C)		0.025	96
	Alumina	7.7 (25-1000°C)		0.027	99.5
	Alumina	~7.3 (25-800°C)		0.022	99.3 (Before Firing)
	Alumina	8.3 (25-1200°C)		0.038	99.9
MRC Superstrate	Alumina	7.3 (25-800°C)	As Fired	0.025	99.6
	Alumina	10.5 (40-400°C)		0.052	-
Kyocera F1330 Union Carbide Oriented Pyrolytic	Forsterite	2.8(c) (300-1100°K)	As Fired	0.038, 0.060	-
	Graphite				
Pemco-Glidden-Durkee P2P36 P3T235	Lithium Aluminosilicate Glaze on Cordierite	~3	As Fired	0.008 - 0.010	-
	Boron Aluminosilicate Glaze on 94% Alumina	~5.5		0.005 - 0.006	-
3M ASM475* ASM614	Zircon (ZrO ₂ · SiO ₂) Alumina	4.9 (25-900°C) 7.9 (25-900°C)	2.0 μm (CLA)**	0.125 0.025, 0.031, 0.035, 0.043 0.028 (Total)	96
	Lead Borosilicate on Alumina	~6.5 (40-540°C)		0.125	-
	Cordierite (2MgO · 2Al ₂ O ₃ · 5 SiO ₂) Alumina	3.7 (25-900°C)		0.125	-
ASM701* ASM772	Alumina	7.7 (25-900°C)	~4.5 μm (CLA)**	0.010, 0.040, 0.043	99.5
	Alumina	7.7 (25-900°C)		0.025	99.9
ASM80F* ASM838	Alumina	7.7 (25-900°)	< 1-2 Microinch	0.005, 0.028	99.5
	Alumina	7.7 (25-900°)			

* Some samples of these materials were received prior to start of contract

**CLA = center line average

ORIGINAL PAGE IS
OF POOR QUALITY

may also be used; for the high-temperature stable ceramics, temperatures up to about 1200°C can be considered, depending upon the properties of the Si-containing compounds in the carrier gas atmosphere.

A thick ($\geq 20\mu\text{m}$) Si film usually is grown on the substrate, in the presence of a small wafer of sapphire; the latter helps in monitoring the test substrate material stability in the carrier gas and growth atmosphere, as revealed by any obvious contamination pattern in the Si growth on at least the part of the sapphire nearest the substrate. The thick Si film also helps to determine if the difference in TEC between the Si and the substrate leads to detectable bowing of the composite due to the differential stresses developed upon cooling to room temperature. Examples of obvious contamination and bowing observed in early studies of Si growth on glasses in He atmospheres are shown in Figures 2-4 and 2-5, respectively.

The Si film also helps reveal certain nonuniformities found in some of the substrates tested, as was evidenced by Si CVD growth on cordierite (Figure 2-6) and on large-grained alumina (Figure 2-7). Incompatibility of the Si with a glaze may also manifest itself in wrinkling of the film-glaze composite after growth, as shown in Figure 2-8. The film was nominally $14\mu\text{m}$ thick in the latter case.

To date both Corning Code 7059 and Corning Code 1723 have been screened for suitability for this program. Both materials were found to be inadequate for the growth of acceptable quality Si by CVD. The bowing of the Code 7059 glass when Si was deposited on it in He at 700°C was too great for it to be a useful substrate for solar cell fabrication (see Figure 2-5). The Code 1723 glass also failed to meet

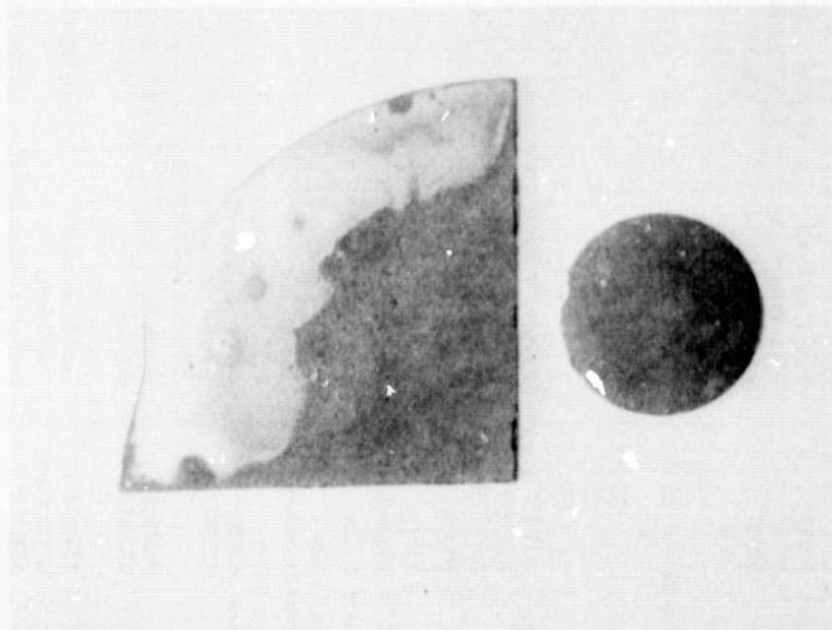


Figure 2-4. Evidence of Contamination of CVD Si Film Growth on Sapphire (Large Wafer) Caused by Nearby Glazed Alumina Substrate (Lead Borosilicate on ASM614) During Deposition in He at 827°C

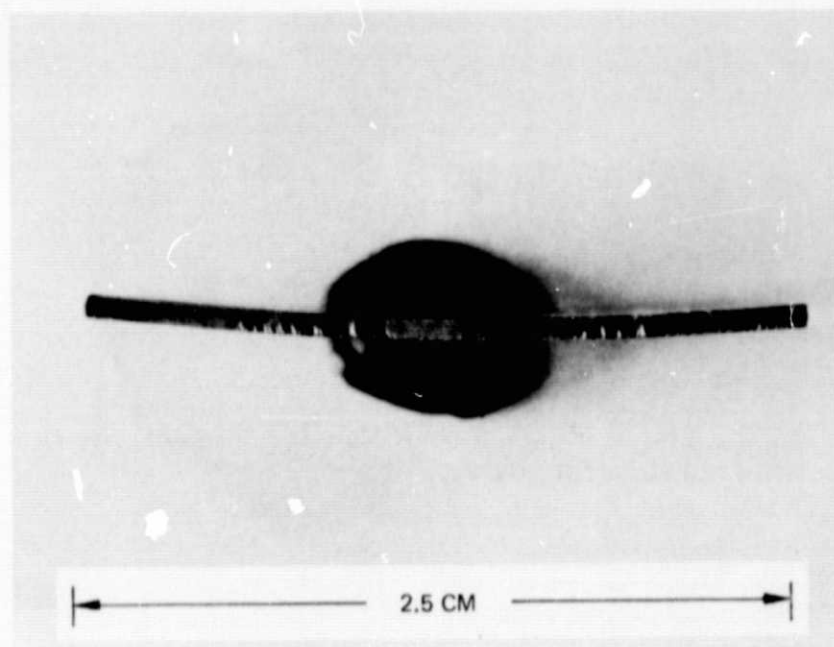


Figure 2-5. Edge View Showing Bowing of Composite of CVD Si on Code 7059 Glass After Deposition in He at 706°C, Si Film on Upper (Concave) Surface

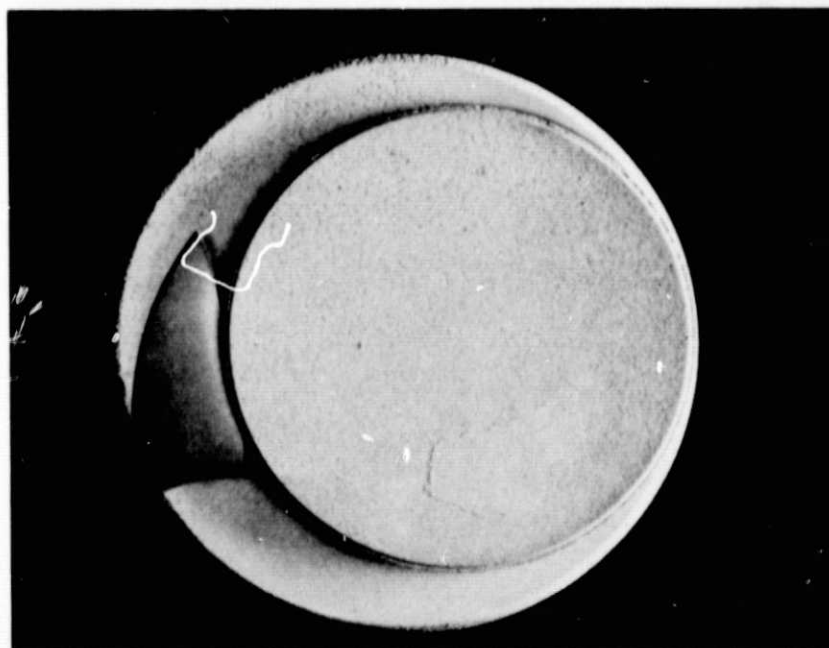
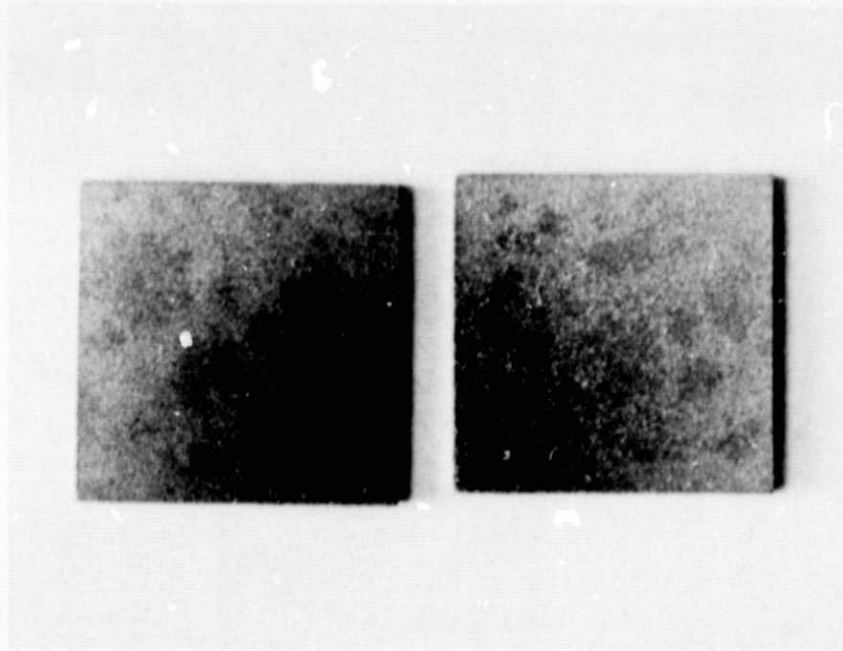
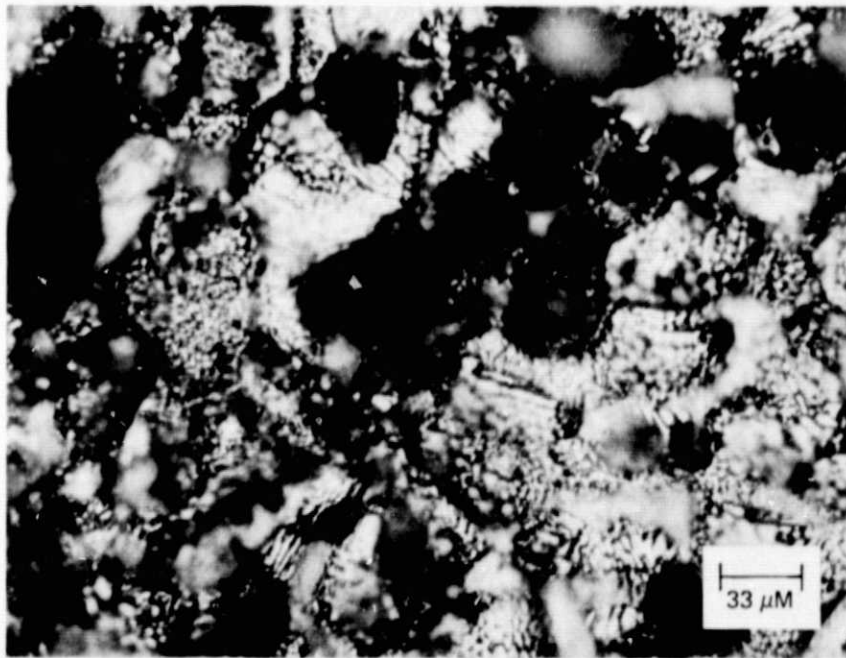


Figure 2-6. Nonuniformity in ASM701 (Cordierite) Substrate Revealed by Si CVD Film Growth in He on 3.5-cm-dia Substrate



(a)



(b)

Figure 2-7. Nonuniformities in Large-Grain Alumina "Tape Product" (Coors), Emphasized by Si CVD Growth, a) Films on 12x12 mm Substrates, b) Photomicrograph Showing Detail of Irregular Grains

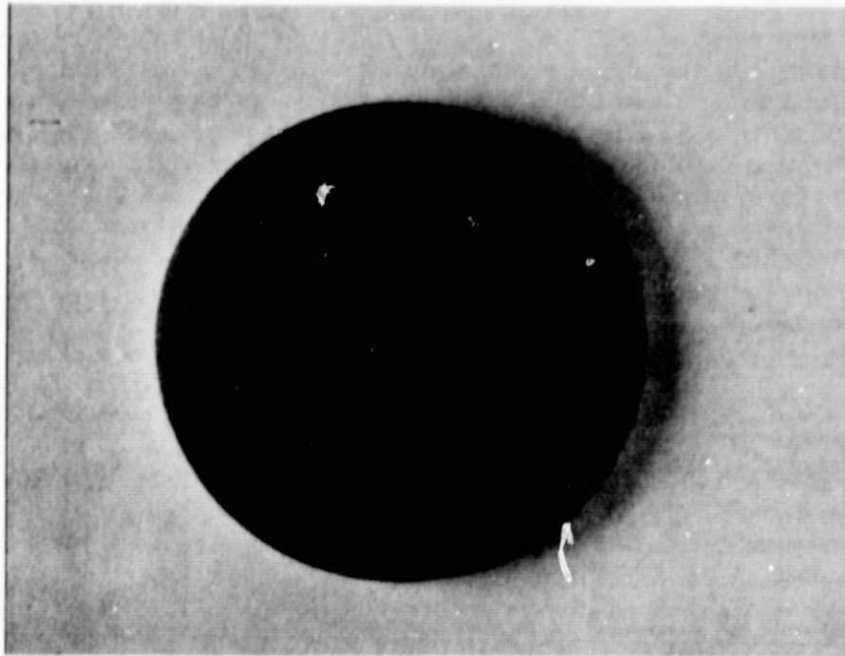


Figure 2-8. Wrinkled CVD Si Film Grown 14 μm Thick on Glazed Alumina Substrate (Lead Borosilicate Glaze 743 on A5M614) in He at 700°C

requirements, mainly due to its thermal instability and/or reactivity with the Si film, even at a temperature as low as 620°C in a He atmosphere. A number of other glasses which were prepared by various vendors specifically for this program have been recently received, and results obtained with them will be given in the next quarterly report.

Preliminary evaluation was also made of a typical alumina substrate (ASM805 from 3M). Si grown by CVD on this material and on sapphire at 1025°C produced single-crystal growth on the sapphire and a film having reflective sheen on the alumina. No obvious form of impurity contamination in the film on the sapphire was in evidence. Based on these preliminary results and the present availability of this and similar substrate materials received from MRC and Coors, the aluminas were selected for some of the first studies of CVD parameters in the work of Task 3.

Characteristics of three polycrystalline aluminas from these manufacturers, some of which were given in Table 2-2, are compared in Table 2-3. Details of the Si growth studies on these substrates are reported in Section 2.3.

Examination of representative samples of these alumina substrates by x-ray diffraction and SEM techniques, described further in Section 2.5, produced some interesting results. Comparison of the principal low-index diffraction line intensities obtained with Cu K-alpha radiation (at 50 Kv and 20 ma) for these samples (all of which consist of corundum, or polycrystalline α -alumina, which is trigonal with

lattice parameters of $a_0 = 4.758 \text{ \AA}$ and $c_0 = 12.91 \text{ \AA}$) with those for a standard random-oriented polycrystalline sample indicated some preferred orientation is present in all three. Specifically, the ADS995 (Coors) shows the strongest preferred orientation, with a tendency for $\{10\bar{1}4\}$ and $\{11\bar{2}6\}$ planes to align parallel to the surface. The ASM805 (3M) also exhibits both $\{10\bar{1}4\}$ and $\{11\bar{2}6\}$ preferential orientation. The MRC Superstrate appears to be the most randomly oriented of the three, although it also has some tendency for $\{11\bar{2}6\}$ planes to be parallel to the surface.

Table 2-3. Representative Properties of Polycrystalline Alumina Ceramics from Three Manufacturers

	ASM805 (3M)	SUPERSTRATE (MRC)	ADS995 (Coors)
Surface Finish (as-fired) (Microinch, CLA*)	1.0 - 2.0	4-5 max	6-10
Surface Crystal Size (μm)	<1.0	~1.5	1-10 (2 ave)
Purity in Al_2O_3	99.9	99.6	99.5
Camber** (inches per inch)	0.003-0.004	0.003 (max)	~0.002-0.003

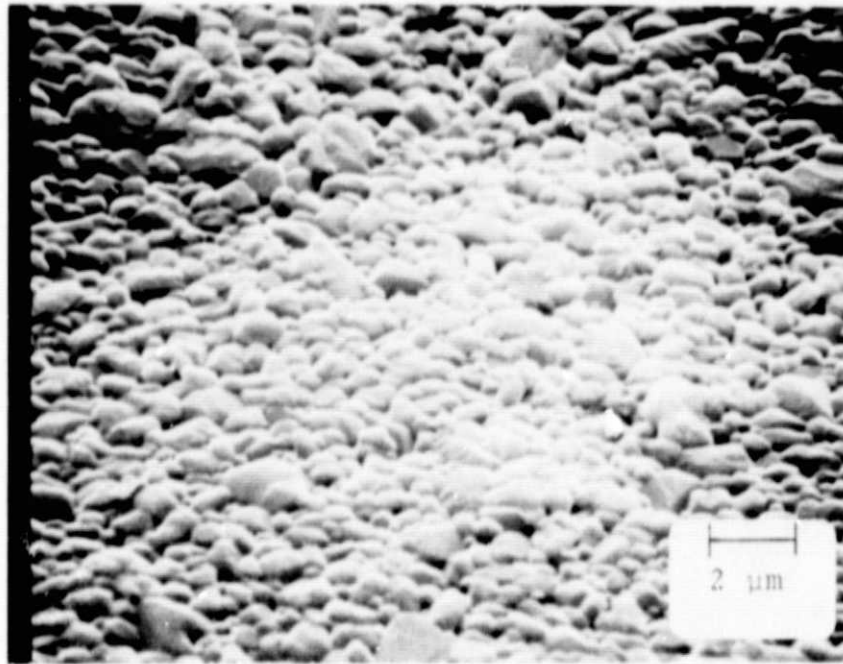
*CLA = Center line average

**Measure of surface curvature of wafer, expressed as amount by which minimum separation of parallel plates through which wafer can pass under its own weight exceeds the nominal thickness, per unit length

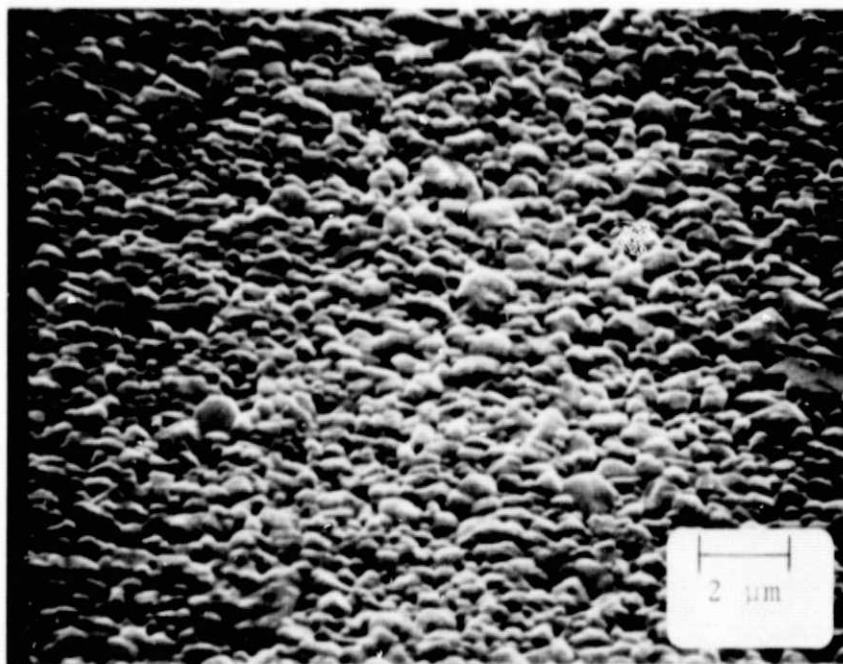
The SEM was utilized to good advantage to examine samples of these same three aluminas. In addition, it had been observed earlier that the ASM805 substrates exhibited a difference in surface smoothness on opposite sides visible to the unaided eye upon careful examination. This difference was readily brought out by surface profilometer traces made on the two sides, using a Sloan Dektak. The SEM photographs in Figure 2-9 demonstrate the difference quite clearly, with the rough side shown in Figure 2-9a and the smooth side in Figure 2-9b.

All three alumina substrates were microscopically rough, with three-dimensional surface features up to $\sim 3 \mu\text{m}$ in height. Figures 2-10a and 2-10b show the MRC Superstrate and the ADS995 (Coors) surfaces, respectively, at approximately the same magnification and the same viewing angle (45 deg) as the photographs of Figure 2-9. The surface morphology is seen to be similar for the four surfaces, but the surface grain size is not. Table 2-4 lists the average size of the surface grains for the three aluminas, as determined from direct measurements on the SEM photographs.

Included in the table is the average surface grain dimension for a separate sample of ASM805 that had been refired by the manufacturer (3M) beyond the normal commercial processing. This material is of special interest because of the much larger apparent grain size, which is shown in the SEM photograph of Figure 2-11.

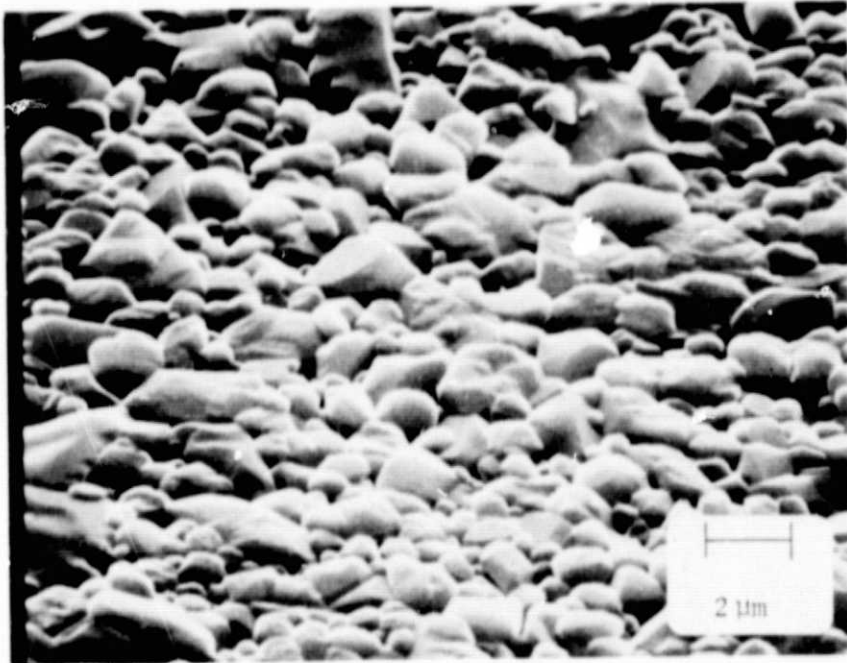


(a)

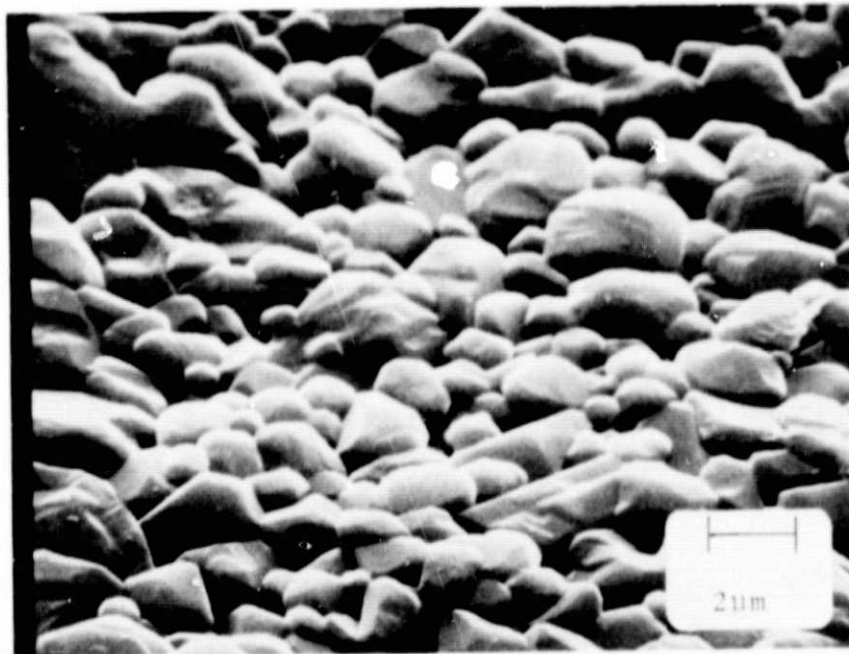


(b)

Figure 2-9. Surface Morphology of ASM805 Fired Alumina Substrate (3M Co.)
a) Rough Side, b) Smooth Side



(a)



(b)

Figure 2-10. Surface Morphology of Fired Alumina Substrates
a) MRC Superstrate, b) ADS995 (Coors)

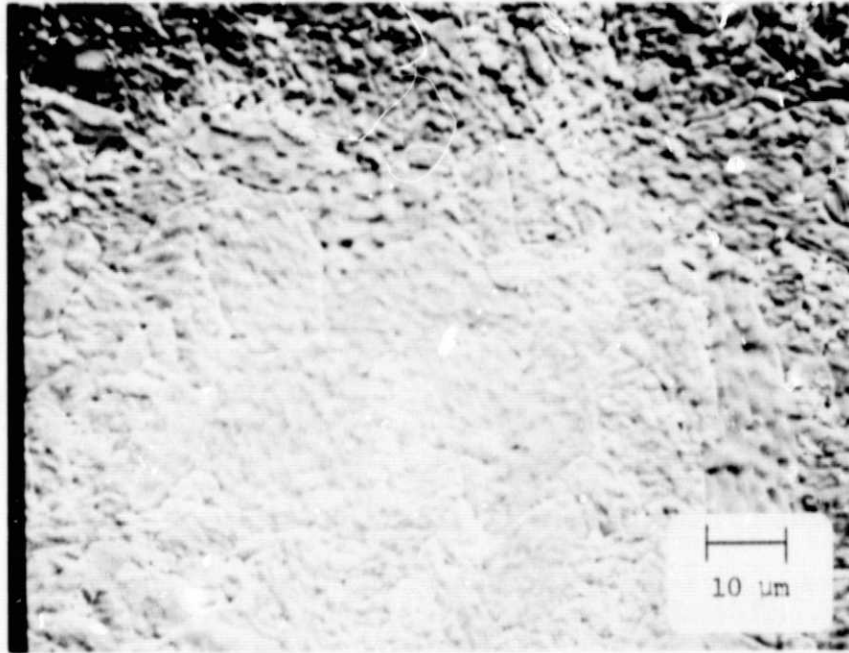


Figure 2-11. Surface Morphology of ASM805 Alumina Substrate Refired by Manufacturer (3M Co.) to Produce Grain Enlargement

Table 2-4. Apparent Surface Grain Size of Several Polycrystalline Alumina Substrates as Measured in SEM

Substrate Material (Manufacturer)	Average Surface Grain Size (μm)
ASM805 smooth (3M)	0.4
ASM805 rough (3M)	0.5
Superstrate (MRC)	1.0
ADS995 (Coors)	1.1
ASM805 refired (3M)	12.5

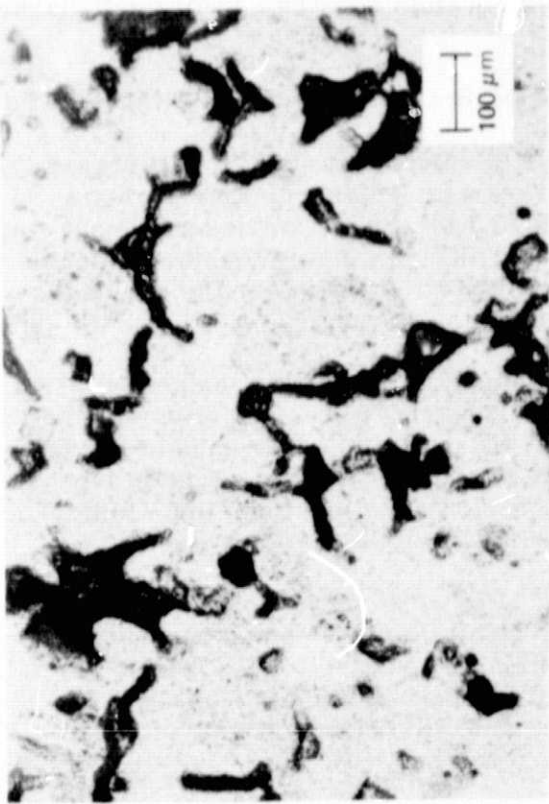
Not only is the apparent grain size quite different but also the entire surface morphology is changed. Si deposition experiments with this substrate material are planned but have not yet been carried out.

2.2.4 Attempts to Produce Improved Substrate Surfaces

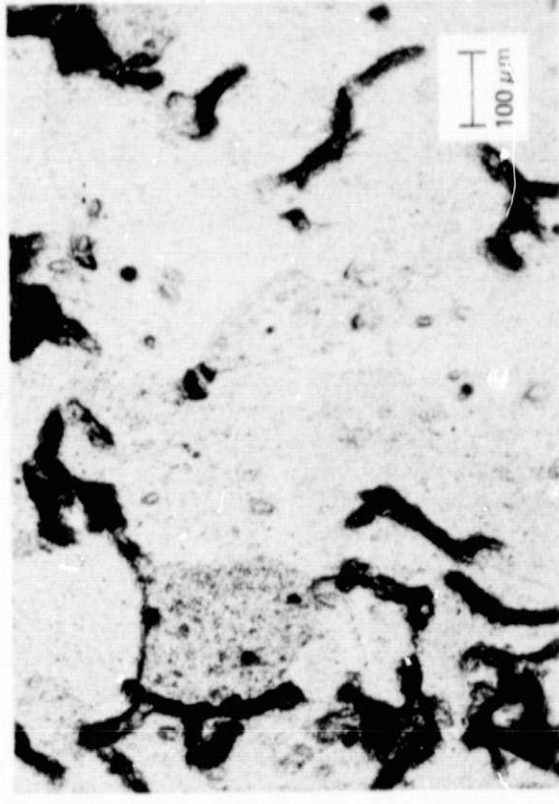
Because of the relatively rough surfaces produced on the fired alumina and other ceramic materials that have been obtained from various manufacturers, several groups of substrates selected from the materials listed in Table 2-2 are being mechanically lapped and polished. The materials included in these groups are the aluminas ASM805 (3M), Superstrate (MRC), and Vistal (Coors), the latter a material that has been subjected to a number of consecutive firings in order to increase the average grain size.

The purpose of this procedure is to generate smooth surfaces on these substrates and yet retain whatever benefits to the Si sheet nucleation and growth process that accrue from the relatively large crystal grains intersecting the mechanically generated surfaces. It is intended that several substrate samples will be extracted from the group at one or more intermediate steps in the lapping/polishing process and be used for Si CVD experiments. This will permit determination of some reasonable balance between the increased cost of preparing substrates by this additional processing step and the expected improvement in the surface characteristics (and perhaps the internal structure) of the resulting polycrystalline Si films.

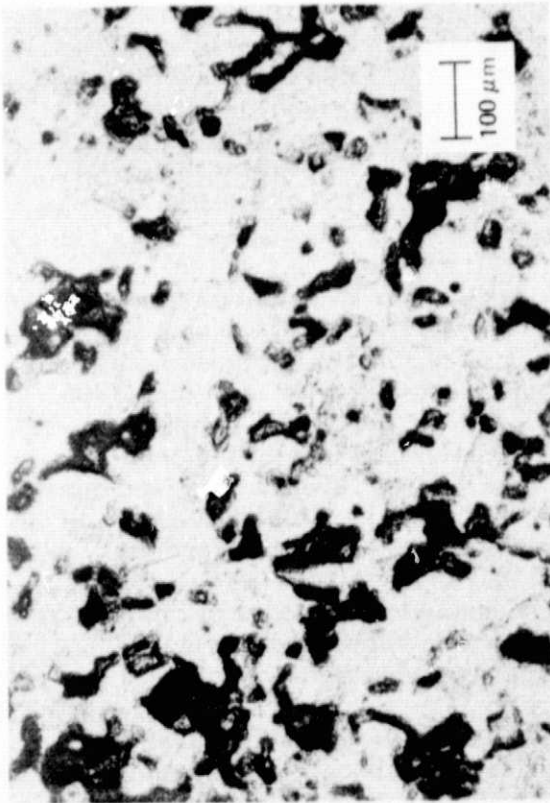
One group of Vistal (Coors) substrates, including several samples of each of four different firing histories, has been lapped for 10 hours with a slurry of $5\mu\text{m}$ SiC particles to produce a flat fine-lapped finish. The four photomicrographs of Figure 2-12, all at the same magnification, show the lapped surface of one of each of the four substrate groups. The prominent irregular crevices intersecting the lapped surfaces on the four samples clearly show the apparent grain growth that has resulted from the consecutive firings, even without any chemical etching. The sample in Figure 2-12a has experienced only a single firing, while those shown in Figures 2-12b, c, and d have been given one, two, and three additional firings, respectively, each at $>1800^\circ\text{C}$ for 6 hours. Other samples of the four groups will be fine-polished before use in Si CVD experiments, but the samples shown in the figure will be used in the lapped condition for exploratory deposition experiments in the near future.



(b)



(d)



(a)



(c)

Figure 2-12. Surfaces of 4 Vistal (Coors) Polycrystalline Alumina Substrates after Successive Firings above 1800°C for 6 Hours.
a) One, b) Two, c) Three, d) Four Firings.

Results obtained on these specially-prepared ceramic substrates will be discussed in the next quarterly report.

2.3 TASK 3. EXPERIMENTAL INVESTIGATION OF SI CVD PROCESS PARAMETERS

Early in the program orders were placed for Si compounds (SiCl_4 , SiHCl_3 , SiH_4 , SiH_2Cl_2) and other materials and supplies (gas regulators, TI-Kote carbon pedestals, He gas, source containers, B_2H_6 in He and PH_3 in He for use as dopant compounds) required for this task. Only SiHCl_3 and SiCl_4 in their source containers have not yet been received, but their use is not contemplated until near the end of the second quarter or beginning of the third quarter of this program.

As noted in Section 2-2, Si deposition experiments performed in the period prior to the contract start date indicated that some of the substrates received from various glass and ceramic manufacturers were reactive in a H_2 atmosphere at the high growth temperatures used -- up to 950°C for a special high-temperature glass supplied by Owens-Illinois and $\sim 850^\circ\text{C}$ for a glazed alumina (ASM743) obtained from 3M. Major contamination was in evidence in films grown on companion pieces of single-crystal sapphire used as control wafers.

Therefore, the use of an inert carrier gas such as He was deemed necessary for studying Si growth phenomena on substrate materials reactive to H_2 . This required carrying out some additional baseline experiments in the vertical reactor system to determine certain characteristics that might differ from those typical of the Si CVD process utilizing H_2 as the carrier gas.

2.3.1 Effect of Carrier Gas Flow Rate on Pedestal Temperature

The horizontal pedestal used in the CVD reactor system is heated by coupling of the rf field of an external coil (see Figures 2-1 and 2-13). The resulting temperature of the surface of this SiC-covered carbon susceptor (pedestal) is non-uniform, the areas near the periphery being hotter than the central region. The differential is greater at high temperatures (e.g., 1025°C) than at the lower end of the region of interest for this work ($\sim 600^\circ\text{C}$), and the average temperature of the pedestal for a given amount of rf power input is affected by the total gas flow rate used.

Some experiments were carried out early in the quarter to establish the magnitude of the effect, for both H_2 and He carrier gases. The temperature of the pedestal in the reactor chamber is measured by means of an infrared radiation thermometer mounted near the chamber, in the arrangement shown schematically in Figure 2-13. Use of the radiation thermometer in position A permits measuring the temperature at any location on the pedestal surface. Corrections for the emittance of the pedestal surface and for losses associated with viewing the hot surface through the fused quartz wall of the reactor chamber are determined experimentally. Normally, during a Si CVD experiment, the pedestal temperature is monitored by viewing the vertical cylindrical surface of the rotating pedestal through one of the spaces between turns of the rf coil (position B in Figure 2-13). The corresponding temperature of the top surface of the pedestal is related to this value by a correction known from previous experimental determinations of corresponding temperatures at both locations.

To measure the effect of gas flow rate on pedestal surface temperatures the observed temperatures were recorded for three different positions on the pedestal and at three different carrier gas flow rates in three different temperature regions,

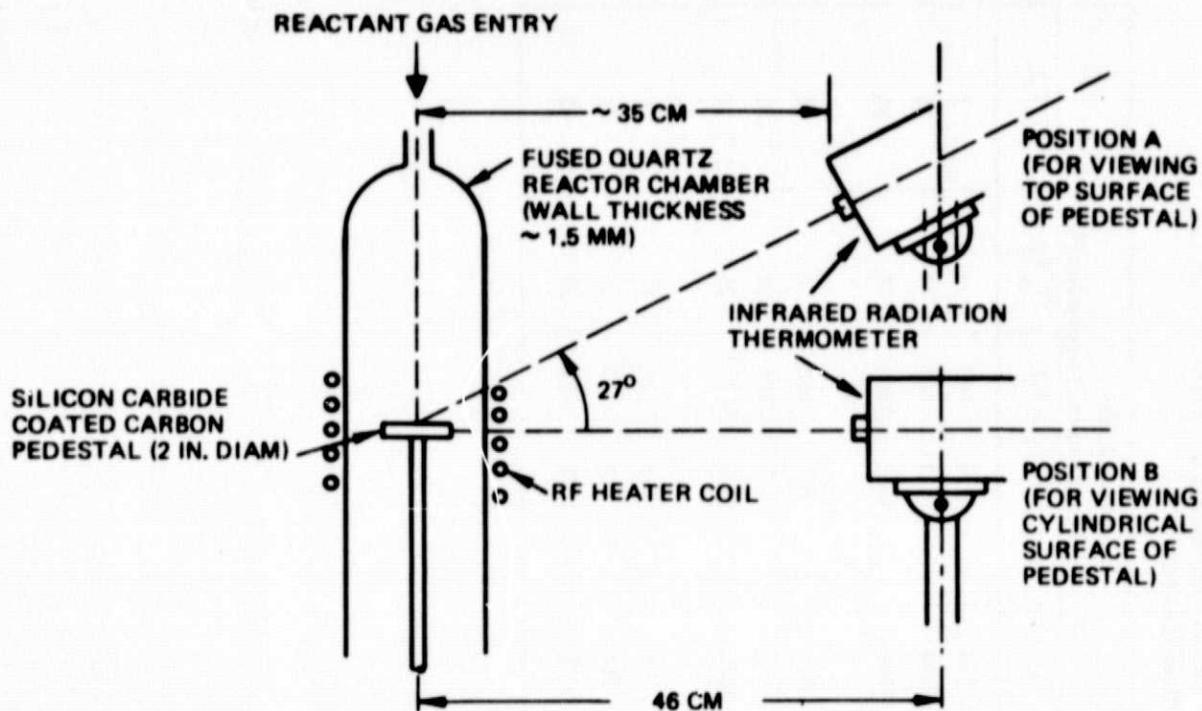


Figure 2-13. Schematic Diagram of Apparatus Arrangement for Measuring Pedestal Temperature with Infrared Radiation Thermometer ($2.0 \leq \lambda \leq 2.6 \mu\text{m}$)

without any Si compound in the chamber and thus no deposition. These temperatures were chosen to be consistent with growth at low temperatures on glasses below their strain points, growth on available glasses just below or near their softening points, and growth on other materials stable at $\sim 1025^\circ\text{C}$. This is the temperature where autodoping from a sapphire substrate, and presumably from polycrystalline aluminas, is still minimal and insufficient to change the observed electrical properties of a single-crystal Si film.

In each temperature region the rf power input to the pedestal was not changed during the observations at the three flow rates; therefore, the differences in temperature at a given location on the pedestal were caused solely by the changes in gas flow rate.

Results of these measurements in terms of observed temperatures are given in Table 2-5 for both H_2 and He carrier gases, for the 5-cm-diameter pedestal now used in the vertical reactor chamber (I. D. $\sim 57\text{mm}$). Inspection of the data for either gas for any one of the three locations on the pedestal shows the expected effect of reduced temperature (i. e., increased cooling of the pedestal) as the total gas flow rate increases. Generally, the magnitude of this cooling effect is similar for the two gases at a given location on the pedestal.

For a given gas flow rate an indication of the temperature profile on the pedestal surface can be obtained from an inspection of the three temperatures T_s , T_t , and T_c in the low-, mid-, and high-temperature regions. This temperature distribution is a consequence of the combined effects of the non-uniform heating of the pedestal/susceptor by the rf field and the several processes of heat transfer away from the

Table 2-5. Observed Temperatures at Three Locations on SiC-Coated Carbon Pedestal (5 cm dia) for H₂ and He Carrier Gases

Carrier Gas Flow Rate (lpm)	H ₂ Carrier Gas				He Carrier Gas			
	T _s *	T _t **	T _c †	(T _s -T _c) / (T _t -T _c)	T _s *	T _t **	T _c †	(T _s -T _c) / (T _t -T _c)
4	590	586	580	10	590	590	583	7
	920	911	893	27	874	877	857	17
	1030	1019	987	43	1053	1042	1008	45
6	566(?)	573	568	-2	571	571	563	8
	911	899	879	33	872	870	850	22
	1024	1012	980	44	1026	1039	1002	24
8	548	549	542	6	555	551	544	11
	857(?)	874	854	3	854	862	835	19
	1012	1002	965	47	1018	1028	985	33

*Measured on vertical cylindrical surface or "side" of pedestal

**Measured on top pedestal surface at distance $d = \frac{3}{4} r$ from center, where r is radius

†Measured at center of top surface of pedestal

pedestal, including heat conduction by the carrier gas moving past the pedestal surfaces.

The temperature difference between the center of the pedestal surface and points approximately three-fourths of the distance from the center to the edge of the top surface is given by the quantity $(T_t - T_c)$ in Table 2-5. This difference is shown in Figure 2-14 as a function of the observed temperature T_c at the center of the pedestal surface, for the three gas flow rates used and for both gases. The results clearly illustrate that the temperature distribution on the pedestal surface depends strongly on the magnitude of the pedestal temperature but is relatively independent of the carrier gas and the gas flow rate.

The difference between the temperature at the center of the pedestal surface--where most substrates are placed for Si CVD experiments--and that observed on the cylindrical side of the pedestal (with the infrared thermometer in position B in Figure 2-13) follows a similar dependence on pedestal temperature. This can be verified by inspection of the values for $(T_s - T_c)$ in Table 2-5. The difference is such that the temperature in the center of the pedestal surface is 8-10 deg C below that of the cylindrical side surface in the low temperature region, about 25 deg C below it in the mid-range, and 40 to 45 deg C below in the high-temperature region. Except where specifically noted, deposition temperatures given in this report are those observed on the side cylindrical surface of the pedestal.

2.3.2 Effect of He Flow Rate on Si Film Thickness Uniformity

Experiments were undertaken to determine a preferred total flow rate of He carrier gas which would lead to acceptable Si film thickness uniformity across the 5-cm diameter SiC-covered carbon pedestal, over a temperature range of 600-1025°C. Total He gas flows of 4, 6, and 8 lpm were used with pedestal temperatures of about 600, 850, and 1025°C, with SiH₄ flows of 25 and/or 50 ccpm. The results are shown in Table 2-6.

Thickness uniformity appeared to be best for 6 lpm at ~850 and ~1025°C and slightly better for 8 lpm at ~600°C. However, a considerable variation in growth rate (as much as ~50 percent) was found across the 38-mm diameter single-crystal sapphire substrates used for the experiments, particularly at ~1025°C. Additional experiments must be carried out to obtain better thickness control in a He atmosphere. Until these experiments are performed, a He flow rate of 6 lpm will be used in growth studies employing the present reactor design, and substrates to be evaluated will be placed at or near the center of the pedestal.

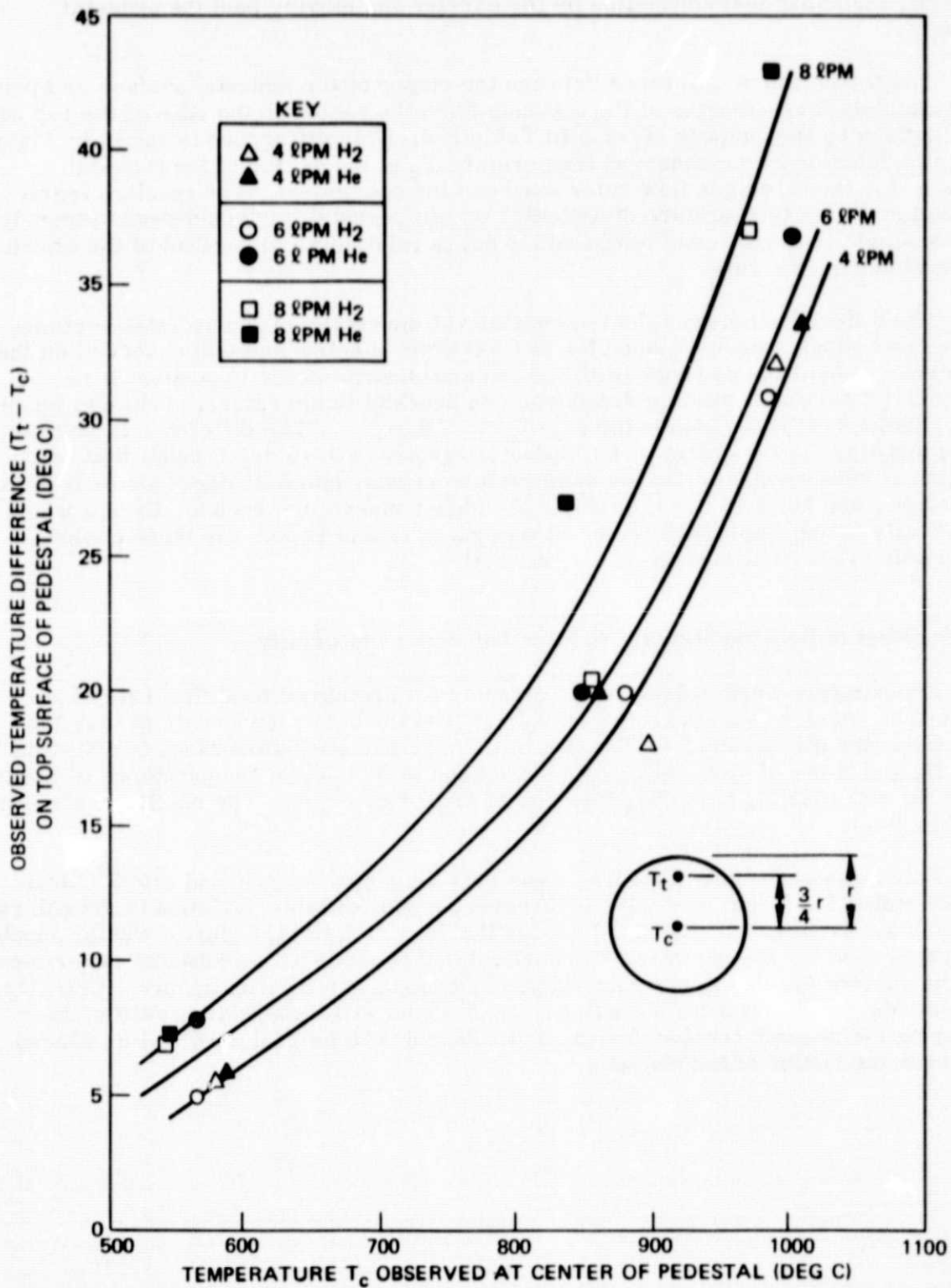


Figure 2-14. Observed Temperature Difference ($T_t - T_c$) on Top of rf-Heated Pedestal for H_2 and He Carrier Gases at Three Different Flow Rates

Table 2-6. Si Film Thickness Uniformity Obtained with He as Carrier Gas
(Single-Crystal (0112) Al₂O₃ Substrates)

He Flow Rate (lpm)	Observed Temp (°C)†	SiH ₄ †† Flow Rate (ccpm)	Deposition Time (min)	Film Thickness (μm)		Growth Rate at Center (μm/min)
				Center	Near Edge*	
4	602	25	10	0.30	0.60; 0.55; 0.45; 0.40	0.03
6	610	25	30	3.2	3.9; 4.1; 4.1; 3.9	0.11
8	596	25	30	2.1	2.6; 2.8; 2.6; 2.4	0.07
4	850	25	6	8.8	4.9; 4.6; 6.6; 6.6	1.5
6	850	25	3	6.6	4.9; 5.2; 4.8; 5.1	2.2
8	853	25	3	7.4	6.2; 5.9; 5.9; 5.4	2.5
4	1025	25	6	1.6	0.7; 0.8; 0.9; 0.9	0.3
6	1025	50	10	16.	11.0	1.6
8	1025	50	5	20.	7; 10; 10; 10	4.0

*These values obtained at 90° intervals near substrate surface periphery

†Temperature observed on side surface of pedestal

††SiH₄ tank no. EN

2.3.3 Effect of H₂ Flow Rate on Si Film Thickness Uniformity

Studies similar to the above were performed with H₂ as the carrier gas, using a SiH₄ flow rate two-fifths as great as was used in the He experiments. The resulting data are recorded in Table 2-7. Thickness uniformity was better than 10 percent across the pedestal for all gas flow conditions. A flow rate of 4 lpm was chosen for use in further growth rate studies when H₂ was used as the carrier gas.

2.3.4 Si Growth Rate as a Function of Temperature

The experiments described in Sections 2.3.2 and 2.3.3 determined the best total carrier gas flow rates from the set 4, 6, and 8 lpm which led to the most uniform film thickness in both H₂ and He over the temperature range 600-1050°C. Using 4 lpm for H₂ and 6 lpm for He, baseline growth rate determinations were made, with (0112) single-crystal sapphire as the substrate and a constant flow rate of SiH₄ (25 ccpm).

For these experiments, a new 1000-gm tank of SiH₄ from 3H Corporation was used. The SiH₄ is reportedly H₂-free (less than 10 ppm); this is important in order to minimize reaction with those substrates reactive with H₂. The only H₂ present when a He or inert atmosphere is used, therefore, will be that generated by SiH₄ decomposition.

The results of these experiments are summarized in Table 2-8 for H₂ as the carrier gas and Table 2-9 for He. The data are also shown in a plot of growth rate vs reciprocal absolute temperature in Figure 2-15. The temperatures used in plotting the data in these curves are corrected temperatures, representing the temperatures of the pedestal surface in regions adjoining the substrates on which Si deposition occurred. Consequently, a determination of activation energies associated with the process of Si layer growth by SiH₄ pyrolysis in H₂ and in He carrier gas atmospheres can be made.

It is clear that different mechanisms are operative in the deposition of Si by SiH₄ pyrolysis in the presence of H₂ and of He. In H₂, a rapid increase in growth rate with increasing temperature occurs for temperatures below about 900°C; above that, the rate still increases with temperature but much less rapidly. The activation energies characterizing the two regions are 1.8 and 0.14 eV, respectively. These results are similar to those reported by other investigators (Refs 4, 5), who report a surface-controlled reaction for Si growth from SiH₄ below 900°C and a mass-transfer-controlled reaction in the temperature range 900-1050°C.

In He, the Si growth rate increase is also rapid at low temperatures (activation energy 1.8 eV), but at about 850°C the growth rate passes through a maximum and then decreases for further increases in the deposition temperature up to at least 1050°C, the highest temperature used to date for these experiments. This maximum in the growth rate at ~850°C may be controlled by appreciable decomposition of SiH₄, caused by radiation, a finite distance away from the hot pedestal, with the formation of silicon hydride polymers (SiH₂)_x which do not efficiently reach the hot pedestal for pyrolysis to form Si. Si formation from (SiH₂)_x is, however, catalyzed by the presence of H₂ (Ref 6).

Table 2-7. Si Film Thickness Uniformity Obtained with H₂ as Carrier Gas
(Single-Crystal (011̄2)Al₂O₃ Substrates)

H ₂ Flow Rate (l per hr)	Observed Temp † (°C)	SiH ₄ †† Flow Rate (ccpm)	Deposition Time (min)	Film Thickness (μm)		Growth Rate at Center (μ m/min)
				Center	Near Edge*	
4	605	10	160	3.5	3.7; 3.7; 3.4; 3.9	0.02
6	605	10	60	0.15	0.10	0.002
4	860	10	5	2.6	2.8; 2.8; 2.5; 2.8	0.52
6	858	10	3	0.80	0.95	0.27
8	855	10	15	3.4	3.6; 3.7	0.23
4	1025	10	1.5	3.0	2.8; 2.5; 2.7; 2.7	2.0
6	1028	10	3	4.1	4.1; 4.0	1.4
8	1030	10	3	5.0	4.5; 4.9	1.7

*These values obtained at 90° intervals near substrate surface periphery

† Temperature observed on side surface of pedestal

††SiH₄ tank no. ER.

Table 2-8. CVD Si Growth Rate Data for Pyrolysis of SiH₄ in H₂ Using (011̄2) Sapphire Substrates*

Observed Temp ** (°C)	Corrected Temp † (°C)	Film Thickness (Center of Pedestal) (μm)	Deposition Time (min)	Ave. Growth Rate (μm/min)
1106	1051	3.7	1.0	3.7
1000	952	2.5	0.75	3.3
952	917	2.7	1.0	2.7
900	865	1.7	1.0	1.7
850	829	1.8	2.0	0.89
750	735	4.5	10.0	0.45
652	641	0.55	6.0	0.01

*H₂ flow rate of 4 lpm; SiH₄ flow rate 25 ccpm (tank No. ER)

**Temperature measured on side surface of pedestal

†Temperatures corrected to values for center of top surface of pedestal

Table 2-9. CVD Si Growth Rate Data for Pyrolysis of SiH₄ in He Using (011̄2) Sapphire Substrates*

Observed Temp ** (°C)	Corrected Temp † (°C)	Film Thickness (Center of Pedestal) (μm)	Deposition Time (min)	Ave. Growth Rate (μm/min)
1106	1051	2.9	4.0	0.72
995	948	5.8	5.0	1.2
952	917	4.0	2.0	2.0
897	872	6.5	3.0	2.2
850	825	3.6	1.5	2.4
807	789	2.4	1.5	1.6
704	691	1.6	10.0	0.16

*He flow rate 6 lpm; SiH₄ flow rate 25 ccpm (tank No. ER)

**Temperatures measured on side surface of pedestal

†Temperatures corrected to values for center of top surface of pedestal

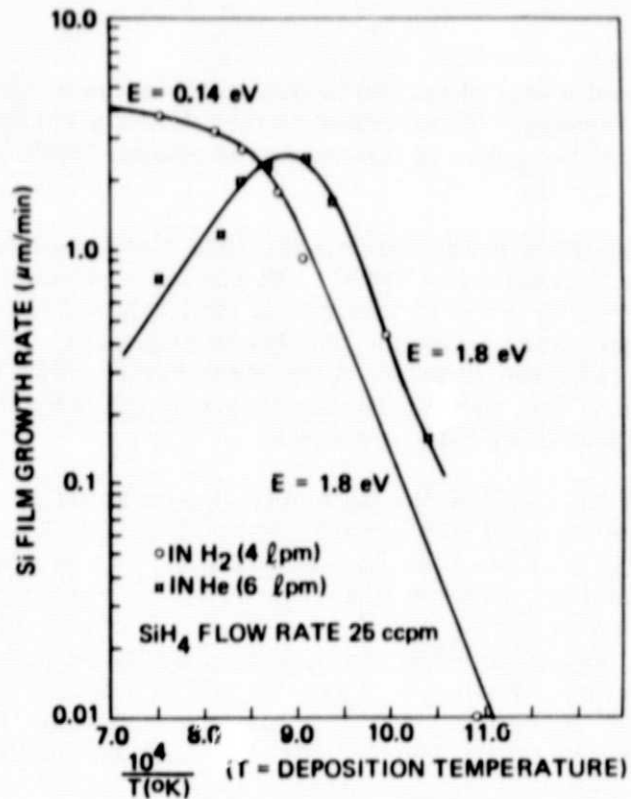


Figure 2-15. Si Film Deposition on (0112) Sapphire Substrates as Function of Reciprocal Temperature for SiH_4 Pyrolysis in H_2 and in He

The differences in growth rate in H_2 and He below 850°C may be due to differences in flow characteristics in the reactor; on the other hand, the somewhat lower growth rate in H_2 in this range may be caused by H_2 adsorption on the substrate surface, thereby hindering SiH_4 adsorption and pyrolysis to Si. Previous studies at Rockwell have demonstrated an increase in Si growth rate at 1025°C when additions of H_2 were made to SiH_4 -He mixtures (Ref. 7). It would be interesting to determine if He additions to H_2 at ~ 800 - 850°C lead to an increase in Si growth rates in that temperature range.

2.3.5 Si CVD on Selected Substrates

Some experiments to investigate the effects of various CVD process parameters --including the properties of the substrate--on the characteristics of the resulting films have been carried out. Three types of substrate have been used--single-crystal sapphire, for baseline reference data; glass; and polycrystalline fired alumina.

2.3.5.1 Si CVD on Glasses

Initial deposition experiments with Corning Code 7059 borosilicate glass (see Table 2-2) were done early in the quarter, prior to the visit to potential suppliers, and at that time deposition parameters were arbitrarily chosen. At a SiH_4 flow rate of 25 ccpm, a He flow of 6 lpm, and a temperature of 700°C , a highly reflective film of Si was grown for 25 min on this glass, but considerable bowing of the film-substrate composite in a concave-upward direction occurred, as was shown in Figure 2-5, indicative of appreciable tensile stress in the film.

However, the composite was observed to bow in the same direction during the growth process, prior to cooling. Thus, other effects directly related to the physical and/or chemical stability of the glass at temperatures around 700°C could be involved.

A second similar experiment showed that the 7059 glass does not distort detectably prior to Si film deposition at 700°C. No bowing was observed in He, for example, at 600, 650, or 700°C after 30 minutes at each temperature, but concave-upward bowing was obvious after only a few minutes of Si growth at 700°C. The distortion therefore resulted from reaction of the glass surface with the SiH₄ or its products of decomposition. This incompatibility may rule out Code 7059 glass as a low cost substrate for Si growth by SiH₄ pyrolysis.

The Corning Code 1723 aluminosilicate material (see Table 2-2) which was specially prepared in plate form (it is normally available only in blown-ware, tubing, and rod form) was recently evaluated for its compatibility with Si grown from SiH₄ in both H₂ and He atmospheres. Si grown in a H₂ carrier at 850°C (~60 deg C below the softening point) resulted in a film with "worm-like" structure, indicating probable local melting or chemical reaction of the glass, and some obvious contamination of the companion sapphire substrate. Bowing was in evidence in a convex-upward direction following deposition, prior to cooling to room temperature, for the 17-μm-thick film on the 750-μm-thick substrate, indicating the film was in compression.

At a growth temperature of 850°C in a He atmosphere, a Si film ~26 μm thick was produced which consisted of a mixture of large and small grains; the Si film grown simultaneously on sapphire gave evidence of having been contaminated by the neighboring glass substrate.

Si growth in He at 650°C, which is just below the strain point of the glass (665°C), produced a very reflective film on the glass, but the film grown simultaneously on the sapphire monitor wafer peeled during handling, suggesting contamination of the Si and/or sapphire by volatile products from the glass. At high magnification, bubbles of various sizes were observed in the Si film and/or at the film-glass interface, by both optical microscope and SEM examination (Figure 2-16). These results indicate that this glass is also probably not satisfactory as a substrate for the growth of Si sheet by SiH₄ pyrolysis.

2.3.5.2 Si CVD on Polycrystalline Alumina

Three companies have to date supplied alumina substrates having smooth surfaces for evaluation for Si CVD growth in this program (Table 2-2). ASM805 from 3M, ADS995 from Coors, and hybrid-grade Superstrate from MRC are all high-purity (99.5-99.9 percent) fired polycrystalline aluminas, properties of which are listed in Tables 2-2 and 2-3.

As indicated in Section 2.2.3, a preliminary evaluation of ASM805 was made early in the program by depositing Si simultaneously on this material and on single-crystal sapphire at ~1025°C by SiH₄ pyrolysis in H₂. The evidence of some crystal faceting in the film on the alumina and the lack of any indication of gross contamination of the sapphire or its epitaxial Si film by the adjacent alumina substrate suggested further work with the fired alumina materials should be undertaken.

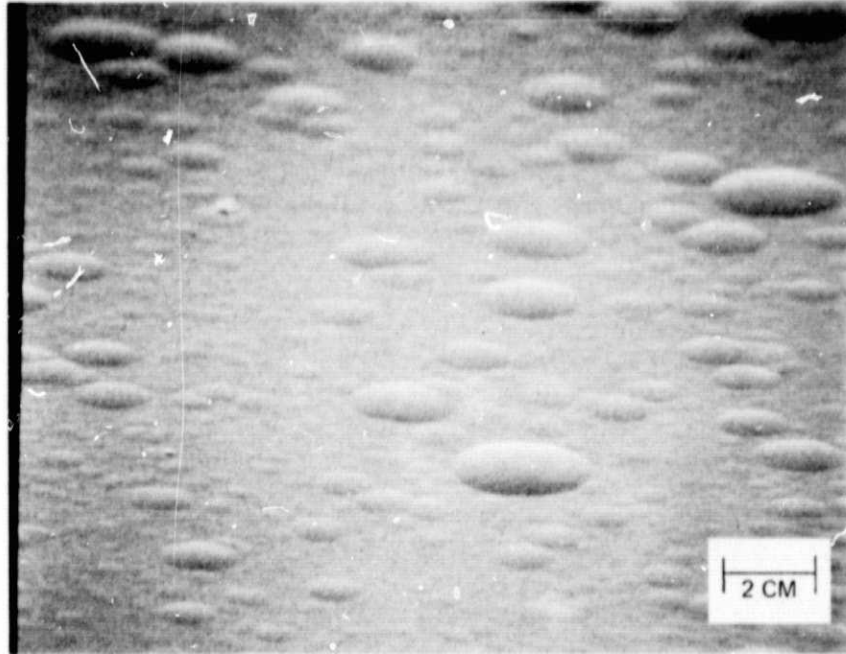


Figure 2-16. Bubbles Formed at Interface of CVD Si Film Grown on Corning Code 1723 Glass Substrate at $\sim 650^{\circ}\text{C}$ in He

The surface roughnesses specified by the manufacturers of the three aluminas listed above range from $0.05\ \mu\text{m}$ for the smoother side of ASM805 to $0.5\ \mu\text{m}$ for ADS995, expressed as an average peak-to-valley height difference (cf Table 2-3). SEM examination of the surfaces of these materials indicated some surface features as large as $\sim 3\ \mu\text{m}$ in height and apparent average surface grain dimensions (in a direction parallel to the nominal surface plane) ranging from $0.4\ \mu\text{m}$ for the smooth side of the ASM805 to $\sim 1.1\ \mu\text{m}$ for ADS995 (Table 2-4).

Films of Si were grown simultaneously on substrates of these three materials. Temperatures of 1025 and $\sim 1100^{\circ}\text{C}$ and carrier gases of H_2 and He were used, to permit a comparison of film structural properties for the several sets of conditions. In each case the film deposition process was preceded by a high-temperature (1250°C) etch in H_2 . The high deposition temperatures were selected to enhance grain growth, with one of the temperatures low enough to minimize any autodoping tendency.

The results obtained in H_2 and in He were quite different. Films $\sim 20\ \mu\text{m}$ thick deposited in H_2 were found to be considerably smoother and more uniform in appearance and in surface roughness than films about $6\ \mu\text{m}$ thick grown in He. The thickness difference for the films grown in the two gases is simply a result of the very large difference in Si growth rate in H_2 and in He at these temperatures (see Figure 2-15).

X-ray diffraction examination of polycrystalline films grown on the three substrates at 1025°C in H₂ (4 lpm) with a SiH₄ flow rate of 10 cpm indicated that {110} preferred orientation was present in all three instances. That is, the individual grains of the polycrystalline films tended to be aligned with <110> directions normal to the film-substrate interface, in varying degrees.

The Si film on ASM805 alumina showed by far the strongest {110} preferred orientation of the three, with the film on the MRC Superstrate alumina next in this regard and the film on ADS995 exhibiting a slight but definite {110} orientation tendency relative to randomly-oriented polycrystalline material.

A similar set of films of comparable thickness grown under the same experimental conditions except for temperature, which was ~1100°C, also were preferentially oriented but in a somewhat different relationship from that found in the films grown at 1025°C. Thus the film grown on ASM805 at ~1100°C still had the strongest {110} preferred orientation of the three, although not as much so as the film grown at 1025°C. However, the film grown on MRC Superstrate at ~1100°C was much less strongly {110} - oriented than at 1025°C, and in fact appeared to have more {111} orientation than a randomly-oriented sample. As was true for the 1025°C group, the film grown on ADS995 also had the least preferred orientation of the three grown at ~1100°C.

It is evident that complex growth patterns are involved in these films that are grown on substrates that themselves have complicated crystalline configurations. More detailed examination of the amount of preferential orientation of a given crystallographic plane that occurs as the growth temperature is varied throughout the range of interest would help to clarify the situation considerably.

The x-ray diffraction evaluation of these two sets of polycrystalline Si films on alumina also indicated that no particle-size line broadening (see Section 2.5) occurred in the films grown on the three aluminas at ~1100°C. However, some evidence of line broadening was observed in two of the films grown at 1025°C. The film on ASM805 did not show the effect, but the film on MRC Superstrate exhibited very slight broadening and that on ADS995 produced significant grain-size broadening. Although the measurements can be considered only as approximate, the average grain size in the Si film on MRC Superstrate may be the order of 0.1 μm while that in the film grown on ADS995 appears to be smaller--the order of 0.04 μm (400 Å). It is interesting that even the relatively small difference in deposition temperature for these two sets of films appears to produce a detectable difference in the average grain size in the Si film in two of the three cases.

The set of films grown in H₂ at 1025°C was also examined in the scanning electron microscope. The film surfaces as grown were nearly identical, all having a rosette-type surface as shown in the SEM photographs in Figure 2-17. The average size of the characteristic surface feature was nearly the same in the three cases--4.2 μm for the film on the MRC Superstrate (Figure 2-17a), 4.3 μm for the film on ADS995 (Figure 2-17b), and 4.1 μm for the film on ASM805 (Figure 2-17c).

However, as shown in Figure 2-18a, the film grown on ADS995 differed in surface morphology from those grown on MRC Superstrate or ASM805 (Figure 2-18b). The latter have a uniformly distributed rosette pattern, whereas the Si film on ADS995 shows non-rosette areas which are clearly faceted crystallographically. This would be expected to be related to a difference in the internal crystal structure of the films. As noted earlier, the principal distinction between the film on ADS995 and the other two, according to the x-ray diffraction analyses, is the much more random orientation of the polycrystalline film grown on ADS995. It is not obvious that a correlation exists between these characteristics; further examination is required.

The results obtained with the ASM805 substrates prompted the preparation of additional relatively thick Si films on other samples of this material, both for further study of the properties of the Si and for use in exploratory solar cell processing (Task 6, Section 2, 6). One set of three films, each grown in H_2 (4 lpm) at $\sim 1025^\circ C$ in separate experiments, was evaluated in some detail. Two of the films were $\sim 20-25 \mu m$ thick, one grown at $\sim 1.6 \mu m/min$ and the other at $\sim 3.3 \mu m/min$. The third film was $\sim 40 \mu m$ thick, grown at $\sim 3.3 \mu m/min$.

X-ray diffraction analysis of the three samples indicated a slight amount of line broadening in all three cases, consistent with the earlier observation of some line broadening for films grown on polycrystalline aluminas at $\sim 1025^\circ C$ but at $\sim 1100^\circ C$. However, in the earlier evaluation the broadening was found in the Si films on ADS995 and Superstrate aluminas but not in the Si grown on ASM805. The results in the three thick films on ASM805 indicate a grain size of about $0.05 \mu m$, similar to the earlier result on the other substrates.

Evaluation of the amount of preferred orientation in this set of three films again established very strong preferred $\{110\}$ orientation in all three, the amount appearing to increase with film thickness, providing confirmation of the tendency of the ASM805 alumina to induce $\{110\}$ Si growth. Also, the thickest film ($\sim 40 \mu m$) gave no $\{100\}$ reflection whatever, whereas in the two thinner ones the $\{100\}$ reflections were relatively stronger than would be observed in a randomly-oriented sample.



(a)

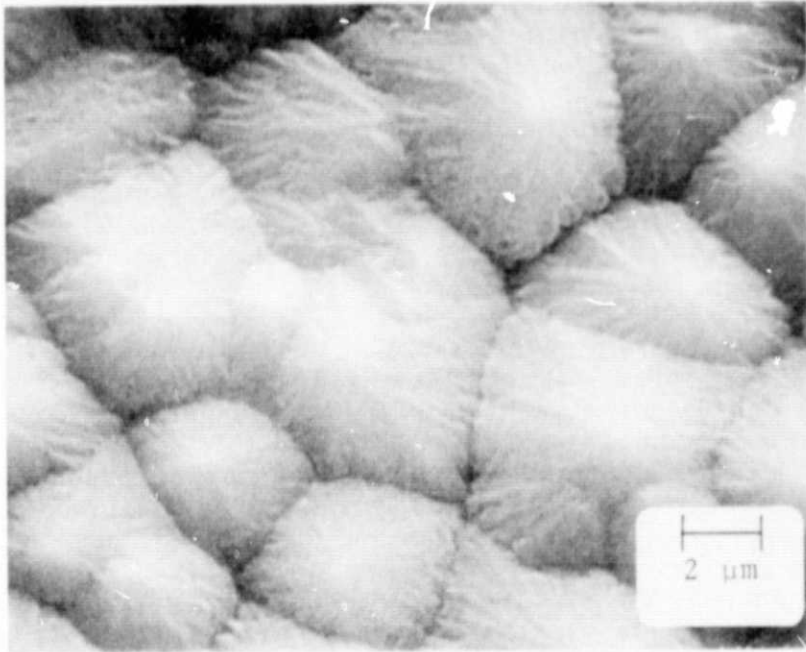


(b)

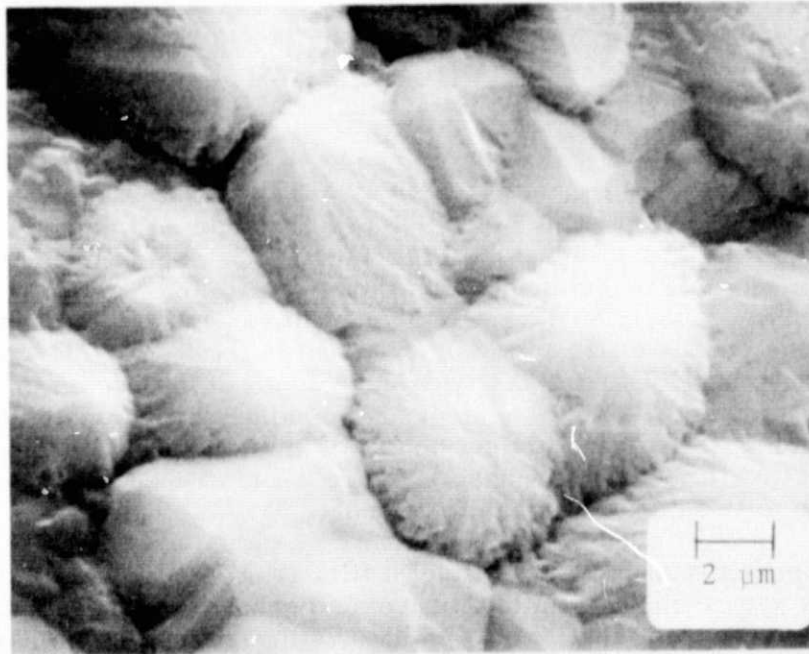


(c)

Figure 2-17. Rosette Surface Structures of CVD Si Films Grown on Fired Polycrystalline Alumina Substrates in H_2 at $1025^{\circ}C$ by SiH_4 Pyrolysis: (a) on MRC Superstrate; (b) on ADS995 (Coors); (c) on ASM805 (3M)



(a)



(b)

Figure 2-18. High Magnification Views of Rosette Surface Structures on CVD Si Films Grown on (a) ADS995 (Coors) and (b) ASM805 (3M), by SiH_4 Pyrolysis in H_2 at 1025°C . Note Faceting in (b).

The same three Si film samples were examined by SEM techniques. The surfaces of the two thinner films, which were grown at rates differing by a factor of about 2, were identical in appearance (Figure 2-19a), with surface rosette features of ~ 3.0 and $\sim 2.8\mu\text{m}$ average dimension for the films grown at ~ 3.3 and $\sim 1.6\mu\text{m}/\text{min}$, respectively. The film grown at $\sim 3.3\mu\text{m}/\text{min}$ to a thickness of $\sim 40\mu\text{m}$ had significantly larger surface features, averaging $\sim 5.2\mu\text{m}$ (Figure 2-19b).

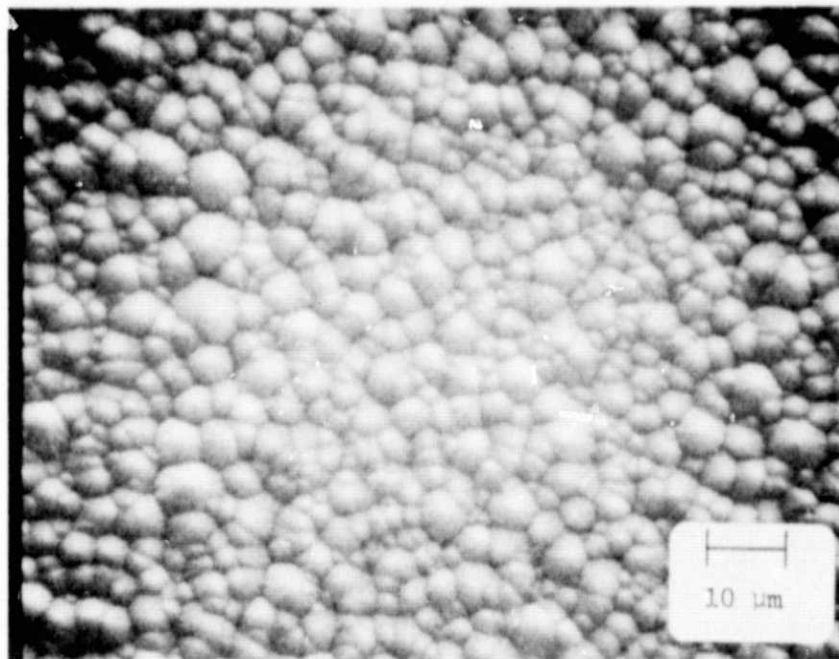
Examination of "cleaved" cross sections of three samples in the SEM showed peak-to-valley dimensions of the as-deposited film surfaces ranging up to $2.5\mu\text{m}$. Typically, however, this dimension was in the range 0.8 - $1.5\mu\text{m}$ for the two thinner films and 1.2 - $1.8\mu\text{m}$ for the $40\mu\text{m}$ film.

As shown in Figure 2-20 the as-broken cross sections suggested columnar growth structure in the films, as well as some kind of transition layer in the part of the film adjoining the alumina substrate, especially in the $40\mu\text{m}$ film (Figure 2-20b).

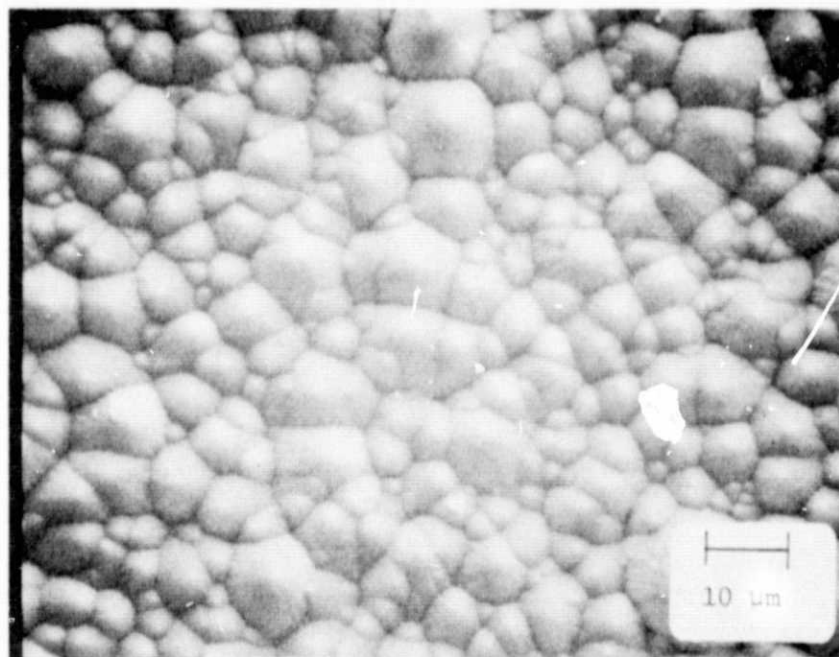
To further elucidate the structure in these films the samples were etched for 1 min. at 65°C in a 1:1 KOH saturated H_2O :isopropyl alcohol mixture. This etch is highly anisotropic, typically etching the $\{100\}$ or $\{110\}$ surfaces 10 to 400 times the rate it etches $\{111\}$ surfaces. After etching, the surfaces revealed the anticipated columnar structure (Figure 2-21). In addition, two other effects were visible. Certain areas exhibited faster etching to form "caves," presently inexplicable. The second effect was that the top half of the film etched significantly faster than the layer adjacent to the alumina interface. This could indicate a significant difference in the average crystallographic orientation of the grains in the upper part of the polycrystalline film with respect to those nearer the alumina-film interface, with the former being more strongly $\{110\}$ -oriented. It might also simply be related to a difference in the etching rate near the interface due to the effect of the nearby Al_2O_3 material.

Another portion of the same $40\mu\text{m}$ film on ASM805 was mounted for a standard metallographic cross section. Following a final step using $0.05\mu\text{m}$ Al_2O_3 abrasive slurry on a silk polishing surface, the sample was etched in the KOH etch at 80°C for ~ 1 min. to delineate structural features. Figure 2-22 shows a region of this cross section both before and after etching, with the polishing scratches visible in Figure 2-22a at an angle of about 45° with the interface. The etching (Figure 2-22b) has delineated the vertical or columnar growth pattern and has also revealed apparent voids or "caves," most of them horizontally disposed and probably the same feature as was observed in the broken cross sections examined in the SEM. The composite photomicrograph shown in Figure 2-23 gives more detail of the region in the center of Figure 2-22, further revealing the apparent columnar growth pattern of the Si film on ASM805 alumina. Finally, examination of this metallographic cross-section sample in the SEM resulted in the photographs of Figure 2-24. These show a nearby region of the cross section at two different magnifications.

The complexity of polycrystalline Si film growth on polycrystalline alumina substrates is very evident from the foregoing discussion. These substrates have produced the most promising results to date, although the preliminary nature of the investigations must be emphasized. The thermal expansion of alumina does lead to some obvious bowing of the Si-alumina composite when films 20 - $100\mu\text{m}$ thick are grown on $625\text{-}\mu\text{m}$ -thick alumina substrates, but these materials offer a means for studying the effects of different growth parameters and processes on Si film properties until an appropriate glass or other material more compatible with Si is found. The present



(a)



(b)

Figure 2-19. Rosette Surface Structures on CVD Si Films Grown on ASM805 Substrates in H_2 at $\sim 1025^\circ C$ at Approximately Equal Rates ($> 3 \mu m/min$).
(a) Film Thickness $\sim 20 \mu m$. (b) Film Thickness $\sim 40 \mu m$.

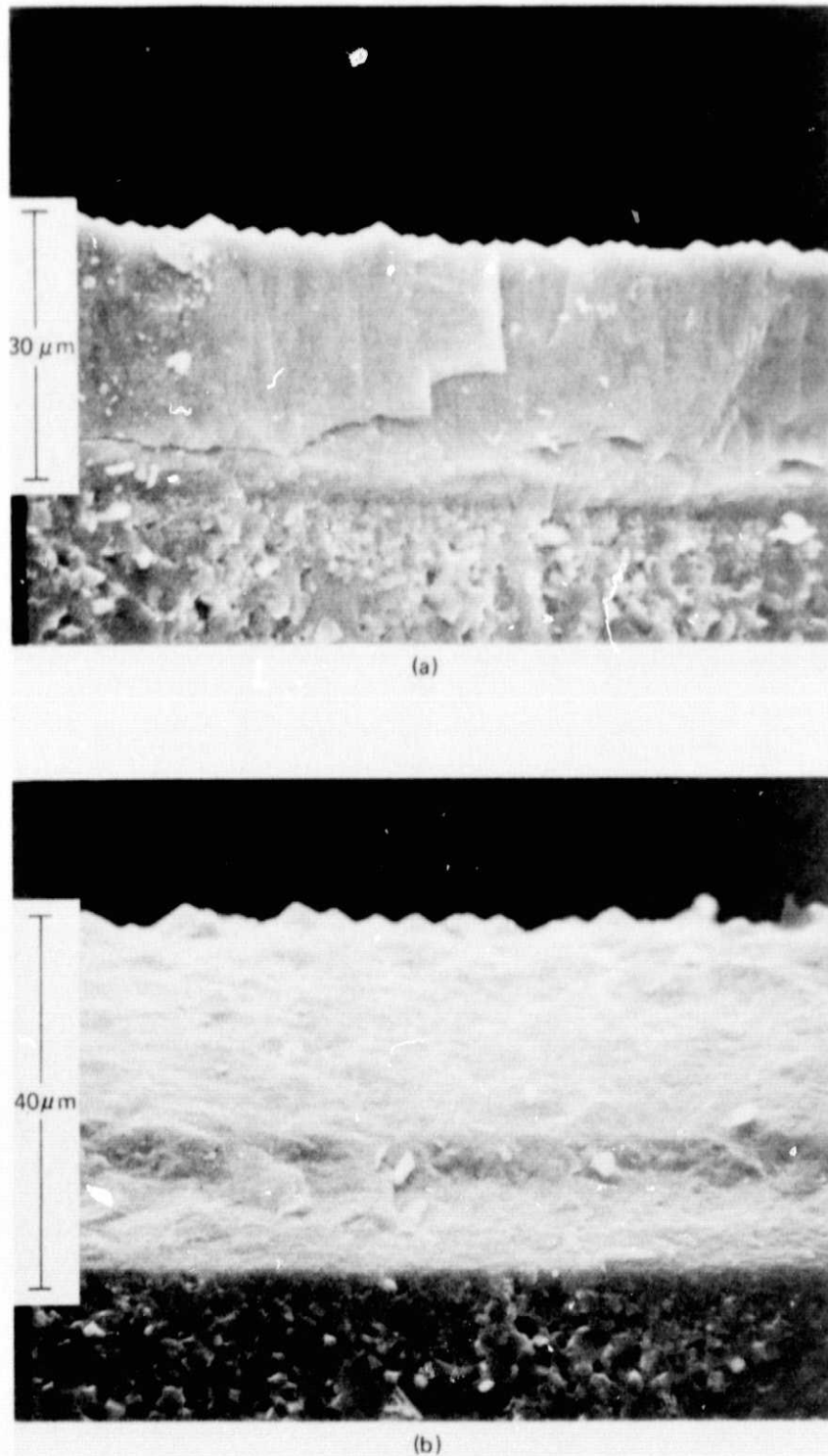


Figure 2-20. SEM Photographs of Cleaved Cross Sections of CVD Si Films Grown on ASM805 Substrates in H_2 at $\sim 1025^\circ C$ at Different Rates. (a) Rate $< 2 \mu m/min$, Thickness 24-30 μm . (b) Rate $> 3 \mu m/min$, Thickness $\sim 40 \mu m$.

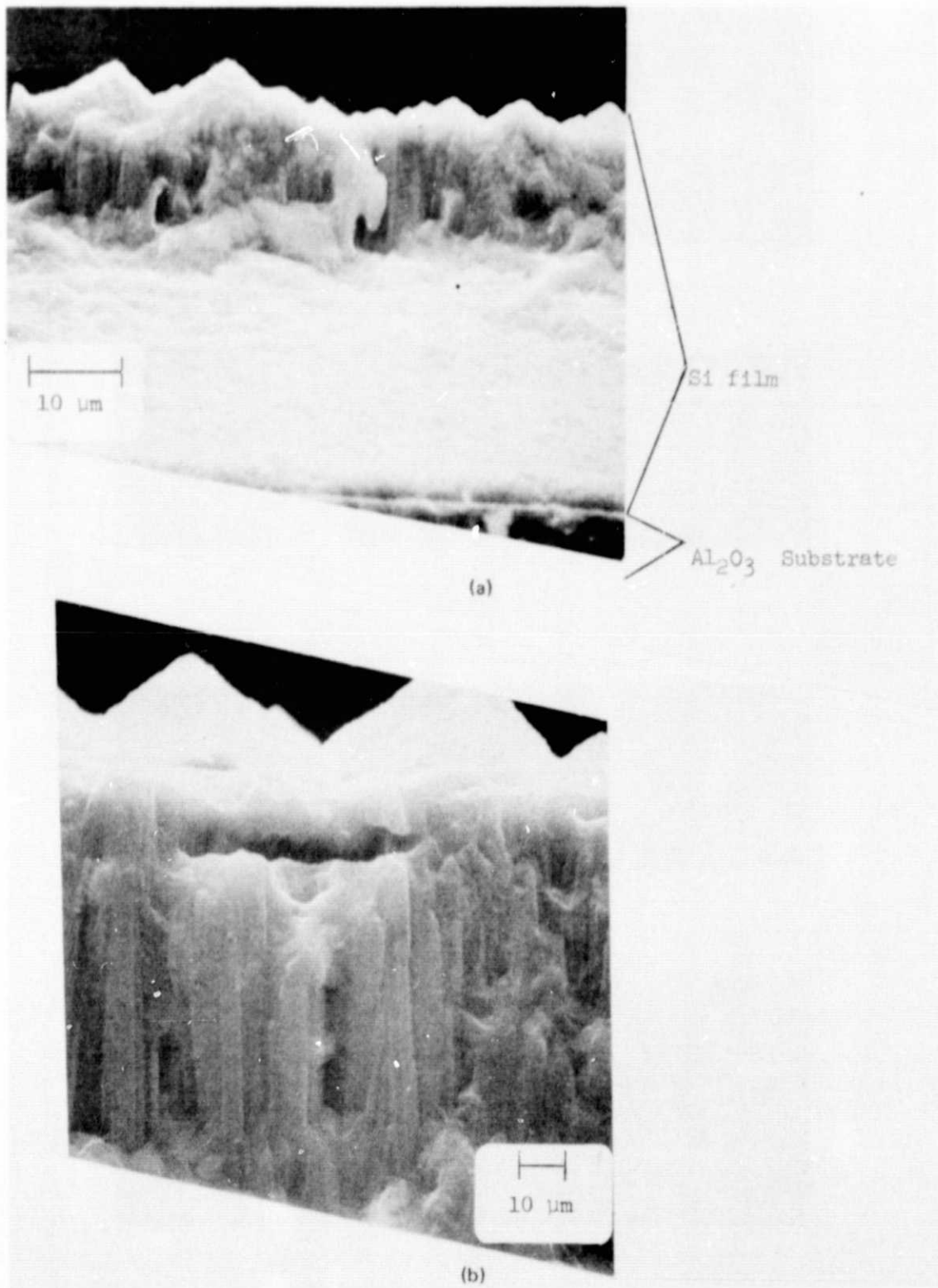
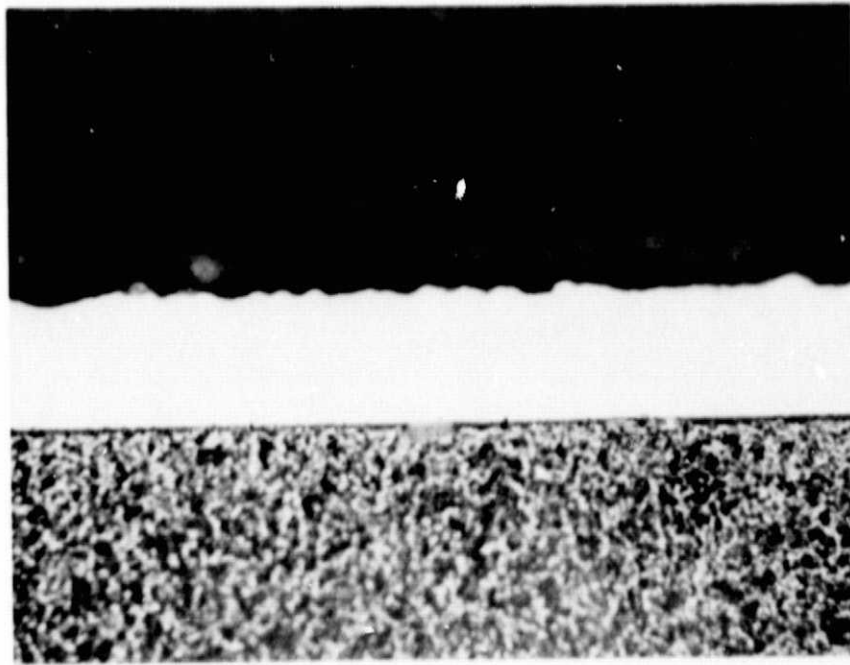
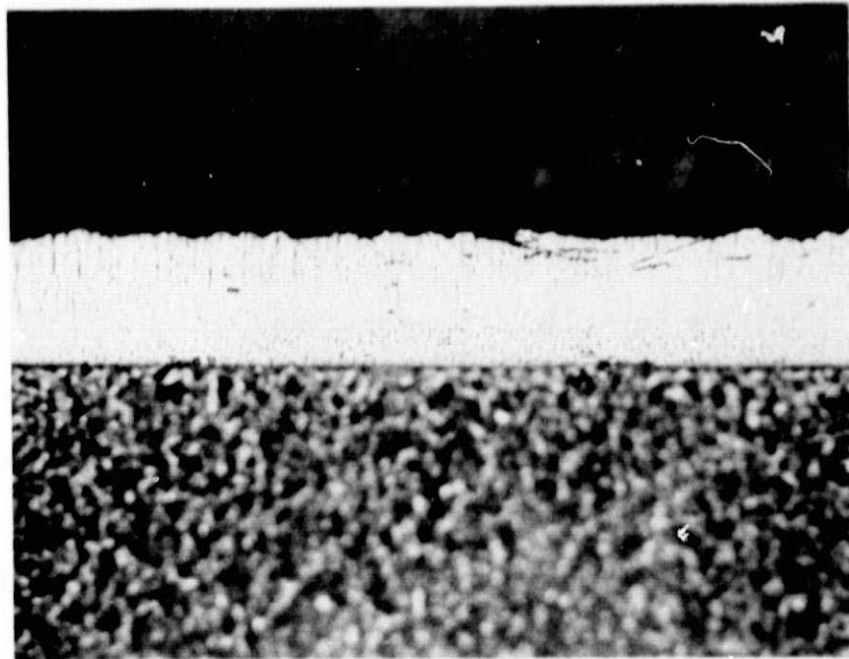


Figure 2-21. Appearance of Cleaved Cross Section of 40- μm -thick CVD Si Film of Figure 2-20(b) After KOH Etching. (a) 1500X, (b) 3000X.

ORIGINAL PAGE IS
OF POOR QUALITY



(a)



(b)

Figure 2-22. Metallographic Cross Section of 40- μm -thick CVD Si Film of Figure 2-20(b). (a) Section After Polishing. (b) Same Region of Polished Section After KOH Etching. (Polycrystalline alumina substrate is at bottom of each photomicrograph.)

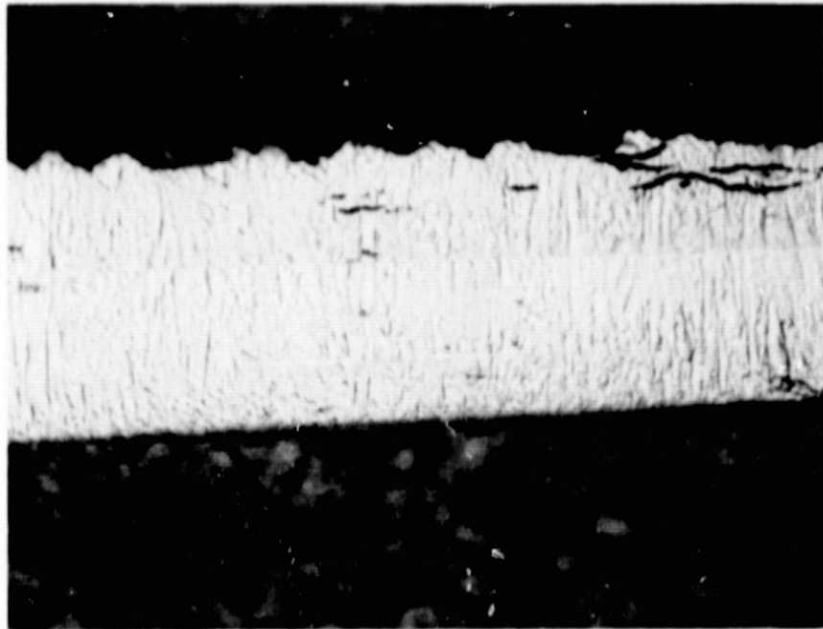


Figure 2-23. Composite Photomicrograph Showing Detail of Central Region of Figure 2-22 (40- μm -thick CVD Si Film on ASM805 Alumina)

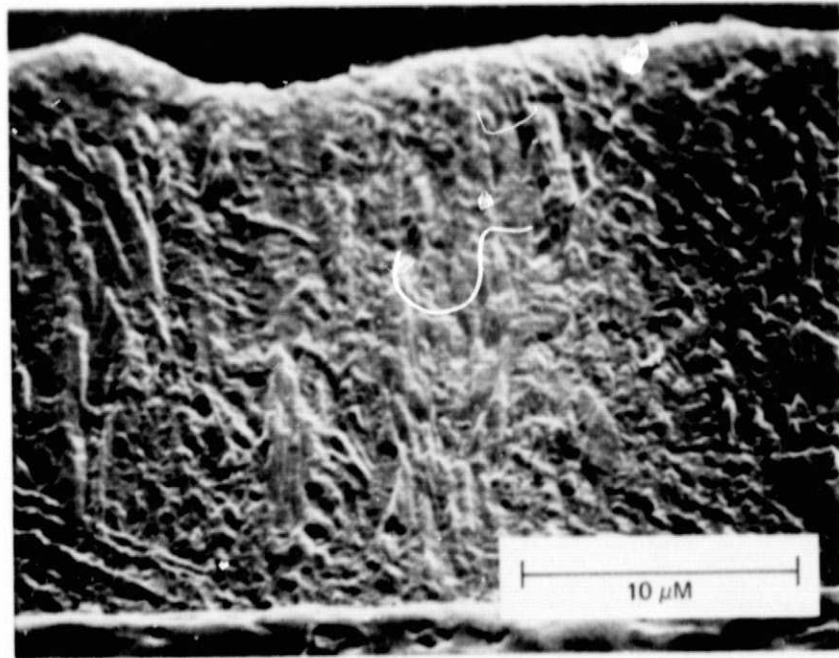
cost of the highest-quality polycrystalline alumina is one-tenth that of polished sapphire substrates in a 5-cm size in large volume purchases. The cost differential is even larger in larger sizes. Cost savings could also be realized as substrate purity requirements are relaxed, the feasibility of which will be determined by the results of film growth studies.

2.3.6 Determination of CVD System Background Doping Level

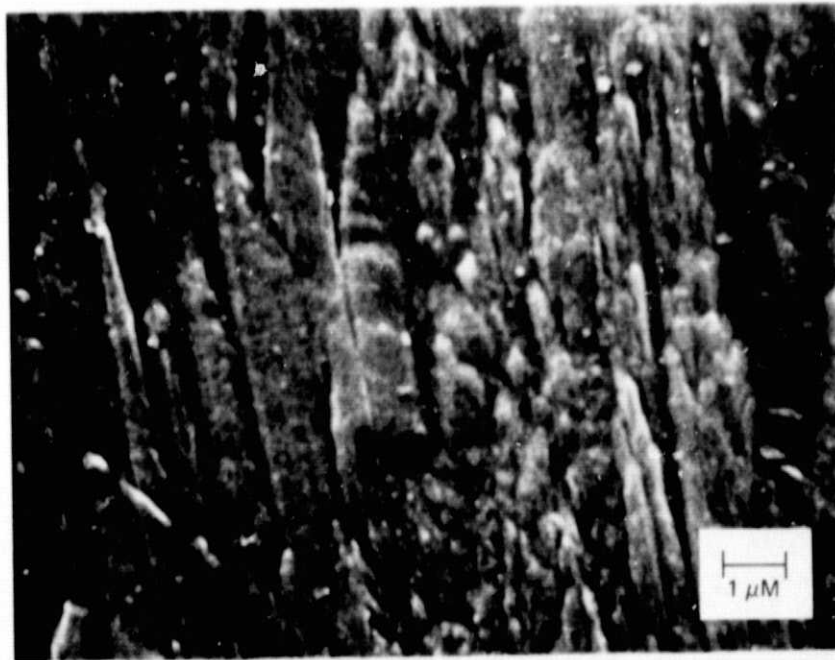
The CVD Si films grown on various substrates up to the time of preparation of this report have not been intentionally doped, although work with doped films will begin early in the second quarter.

Electrical measurements have been made on several of the undoped epitaxial Si films prepared to date, by both the van der Pauw and the conventional Hall-bridge methods. The films were grown on single-crystal (01 $\bar{1}2$)-oriented polished sapphire and on high-resistivity single-crystal Si substrates, the former at temperatures of 1025 and 1100°C and the latter at 1025°C in H₂ and in He carrier gases.

Results of these measurements indicate that the undoped films are p type, with the carrier concentration typically $\sim 10^{15}$ cm⁻³. More precise determination of this background doping level will be made on epitaxial undoped films grown after the reactor system modifications are completed, early in the second quarter.



(a)



(b)

Figure 2-24. SEM Photographs of Metallographic Cross Section of Figures 2-22 and 2-23 at (a) 3750X and (b) 7550X for CVD Si-on-ASM805 Alumina Sample of Figure 2-20, Showing Apparent Columnar Growth

2.4 TASK 4. PREPARATION OF SI SHEET SAMPLES

The work of Task 4 is entirely in support of the activities of Tasks 3, 5, and 6. It consists primarily of the preparation of individual samples or groups of samples of CVD Si on various substrates, utilizing well-established deposition procedures. These samples are mainly for use in film characterization studies (Task 5) to examine the variation in Si properties with systematic deposition parameter variations or for use in fabrication of exploratory solar cell structures at OCLI (Task 6). Occasionally, special samples of a non-routine nature are prepared which nevertheless do not require extensive exploratory evaluation of the interdependence of CVD parameters on the resulting properties of the films, and such work is also a part of this task. Any samples prepared strictly for demonstration purposes are also considered part of this task.

The task is as much an administrative convenience as a separate technical activity, and therefore will not receive separate attention in this report except for the observation that approximately 60 Si CVD experiments were carried out in the first quarter, in addition to about 15 other experiments in the CVD reactor that did not result in the growth of a Si film. Of the former, only about six of the runs made with the reactor system were considered to be of a routine nature and thus to be part of the Task 4 activity.

2.5 TASK 5. EVALUATION OF SI SHEET MATERIAL PROPERTIES

The Technical Program Plan (see Appendix B) called for only limited activity for this task prior to the second month of the contract. In the first month preliminary investigation of x-ray diffraction techniques for grain-size determination by line broadening was undertaken, and attempts were made to obtain standard reference samples of Si in a range of particle sizes, to provide an experimental calibration for the x-ray method.

As the experiments of Task 3 began to produce a variety of CVD Si films on several types of substrate, the film (and substrate) characterization activities of this task accelerated considerably. Much of the work has already been reported in the discussion of Task 3 (Section 2.3), but some additional details will be given here.

2.5.1 Measurement of Surface Topography (Roughness) of Films and Substrates

A wide range of surface topography is represented by the three main types of substrate materials expected to be used in the early stages of the contract work--namely, glasses, glass-ceramics, and polycrystalline aluminas and similar fired ceramics. The surface of a film deposited on a substrate usually has a topography directly related to that of the substrate, especially if the latter is heavily textured. In addition, if epitaxial growth occurs in the film the characteristics of its surface will be further influenced by crystallographic features resulting from the nature of the growth. In any case, it is important to know the nature and magnitude of the surface irregularities on a substrate as well as on the deposited film. Optical microscopy and photomicrographs, SEM examination, and surface profilometry are among the methods used to characterize these surfaces.

A Sloan Dektak has been used for measurement of surface roughness and details of other topographic features; it has also been used for film thickness measurement when an abrupt step from film to substrate can be formed by removal of the Si film by masking and etching procedures.

Surface profilometry was used to examine and record the surface finish on several of the fired polycrystalline alumina substrate materials of interest, including the three used in the CVD parameter study described in Section 2.3.5.2. This procedure is useful for the rapid screening of substrate surfaces to provide both a qualitative overall view of the surface finish and a quantitative measure of localized surface features. It is expected that such profiling will be carried out routinely on both the initial substrate surface and the deposited Si film surface in the early stages of the program.

The Dektak sensitivity scale and traverse rate used for a given surface must be a compromise based on the actual vertical (and horizontal) dimensions of the surface features and the ability of the probe stylus to follow the contour of these features. The probe stylus has a radius of $12.5\mu\text{m}$, with a tracking force of 50 mg. The vertical deflection sensitivity ranges up to a maximum of 10\AA per mm spacing on the recorder paper, although the highest sensitivity range found practical is 50\AA per mm.

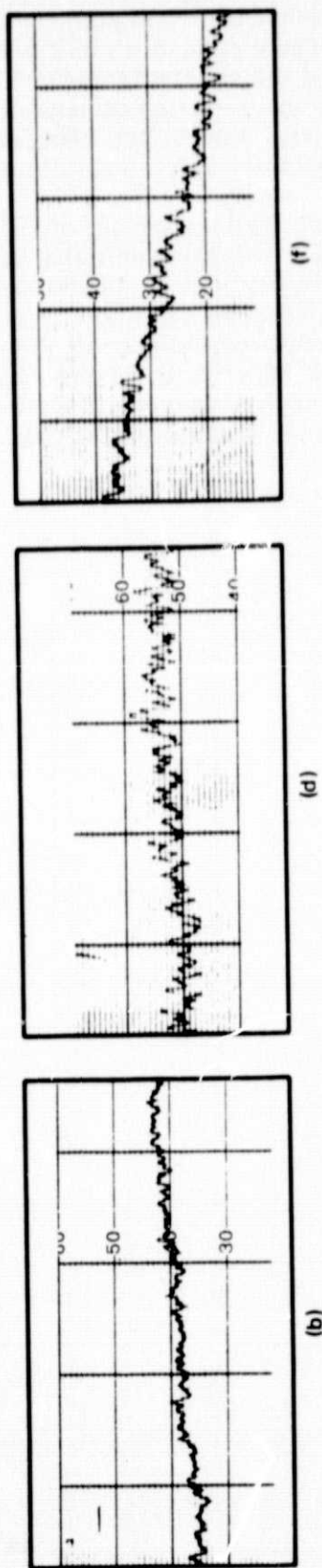
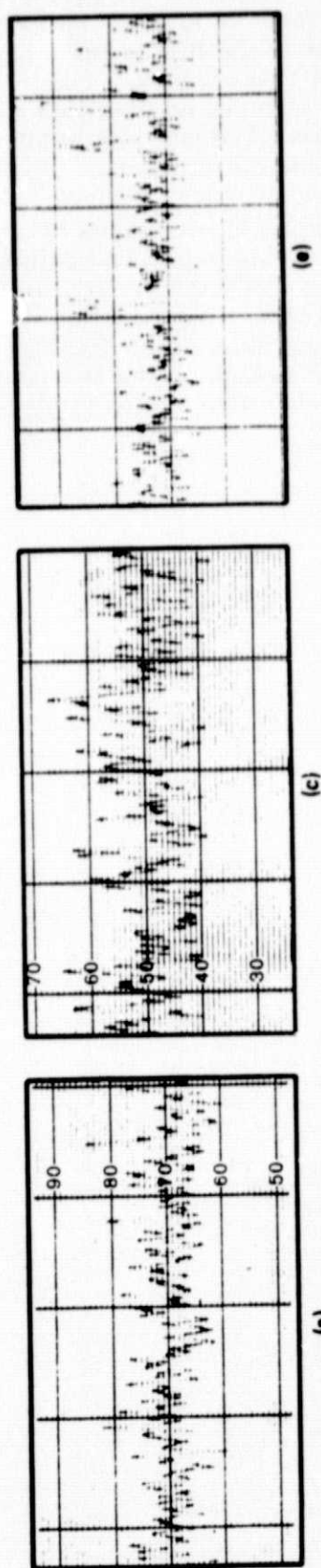
The average surface roughnesses of the three as-fired aluminas referred to above, expressed as an average vertical peak-to-valley difference, were found to be as given in Table 2-10. Also given in the table is the measured roughness of the refired ASM805 alumina from 3M that was examined in the SEM and described in Table 2-4 and Figure 2-11, and which exhibits an apparent surface grain dimension (horizontal) of about $12\mu\text{m}$ (cf Table 2-4).

Table 2-10. Average Measured Surface Roughness of Polycrystalline Alumina Substrates Measured by Surface Profilometry with Sloan Dektak

Substrate Material (Manufacturer)	Average Vertical Peak-to-Valley Dimension (μm)
ASM805 smooth (3M)	≤ 0.1
ASM805 rough (3M)	~ 0.25
Superstrate (MRC)	~ 0.15
ADS995 (Coors)	~ 0.35
ASM805 refired smooth (3M)	≤ 0.1
ASM805 refired rough (3M)	~ 0.26

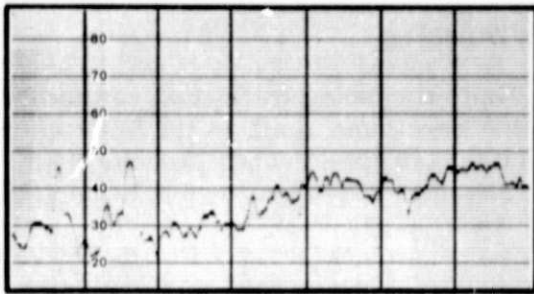
Figure 2-25 shows representative segments of Dektak traces for the surfaces of the three alumina substrates and also for the as-grown surfaces of Si films on them in H_2 at $1025^\circ C$. The extent to which the surface roughness of the film is influenced by the topography of the substrate surface is emphasized by these traces. The apparent average peak-to-valley dimensions of the surface features on the films are ~ 0.7 , ~ 1.0 , and $\sim 0.6 \mu m$ for the films on MRC Superstrate, ADS995, and ASM805, respectively, although the latter exhibits some extreme vertical excursions.

Figure 2-26 shows another set of Dektak traces, obtained at two stages of preparation of the Coors Vical alumina substrates that are being lapped and polished for use in Si CVD experiments. These substrates have been subjected to successive firing sequences to enhance grain size; the surfaces of representative samples of each of the four groups were shown in Figure 2-12 after completion of the lapping process. Figures 2-26 a, c, e, and g show segments of the Dektak traces obtained for the surfaces of each of these substrates in the as-fired condition, while Figures 2-26 b, d, f, and h show the surfaces after the lapping step.

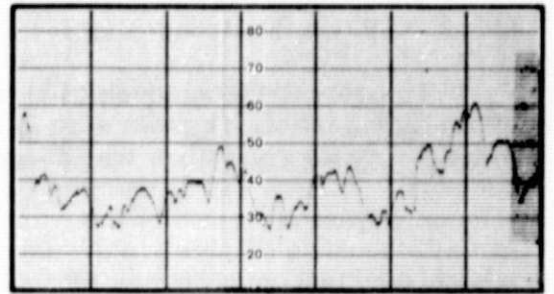


NOTE: ALL VERTICAL SCALES 0.1 μm /DIVISION

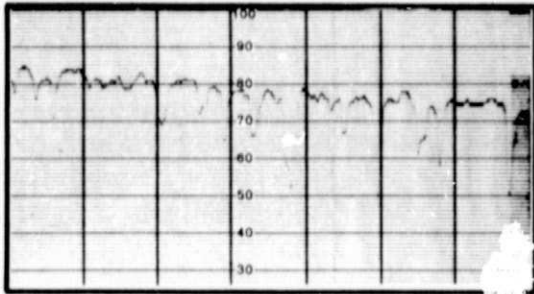
Figure 2-25. Dektak Profilometer Traces for As-Fired Surfaces of Polycrystalline Alumina Substrates and for As-Grown Surfaces of CVD Si Films (SiH_4 Pyrolysis in H_2 at 1025°C) on Each. (a) 26- μm -thick Si on (b) Superstrate (MRC); (c) 17- μm -thick Si on (d) ADS995 (Coors); (e) 27- μm -thick Si on (f) ASM805 (3M), Rough Side.



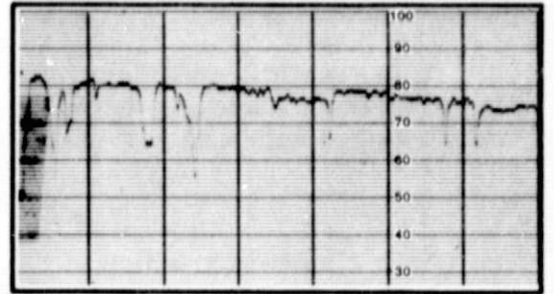
(a)



(c)

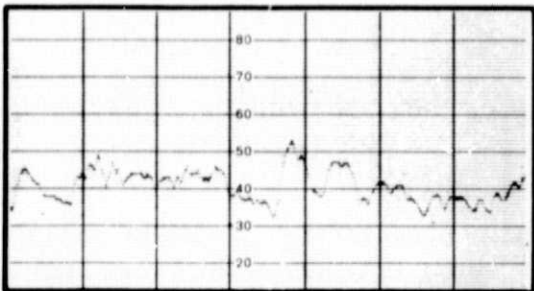


(b)

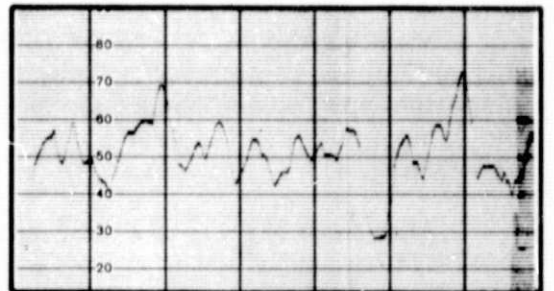


(d)

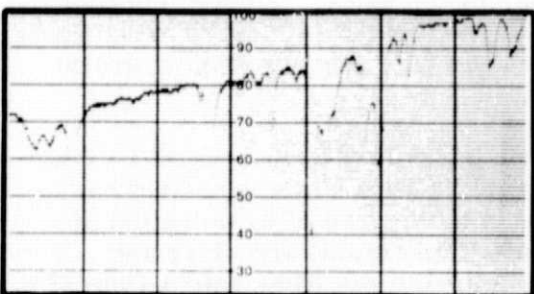
NOTE: ALL VERTICAL SCALES ON a, c, e AND g ARE 0.5 μm/DIVISION
NOTE: ALL VERTICAL SCALES ON b, d, f AND h ARE 0.1 μm/DIVISION



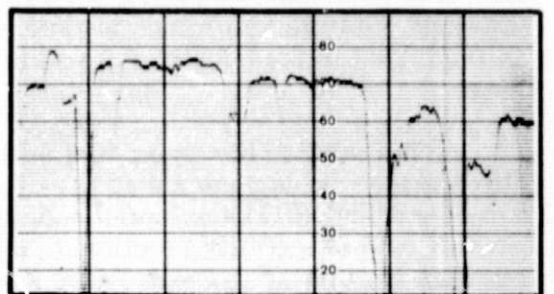
(e)



(g)



(f)



(h)

NOTE: ALL VERTICAL SCALES IN BOTTOM ROW ARE 0.1 μm/DIVISION

Figure 2-26. Dektak Profilometer Traces of Surfaces of Vistal (Coors) Polycrystalline Alumina Substrates Subjected to Four Different Firing Histories. Single Firing, (a) Before, (b) After Lapping; Two Firings, (c) Before, (d) After Lapping; Three Firings, (e) Before, (f) After Lapping; Four Firings, (g) Before, (h) After Lapping.

2.5.2 X-Ray Line Broadening for Grain Size Determination

To apply the techniques of x-ray diffraction line broadening to the determination of average particle or grain size in a polycrystalline specimen, such as the Si films prepared under conditions that do not produce epitaxial (single-crystal) growth, it is necessary to know the diffraction line width in the absence of any grain-size broadening effects. This line width is the combined result of the true diffraction line width - which is finite because of such factors as non-perfect crystals, imperfectly collimated x-ray beams, and non-monochromatic incident radiation - and instrumental line broadening, associated with factors such as the width of the effective x-ray source in the particular diffractometer used.

It is generally considered that grain sizes in excess of $\sim 0.1 \mu\text{m}$ do not produce any x-ray line broadening due to crystal size effects alone. Thus, the diffractometer trace obtained with a polycrystalline sample containing randomly oriented grains or particles significantly larger than $\sim 0.1 \mu\text{m}$ should provide a measurable reference line width free of size broadening effects, i. e., with zero grain-size broadening.

Such a zero-broadening Si sample was prepared by grinding single-crystal (Czochralski) wafers with an agate mortar and pestle. The resulting charge was then passed through a No. 140 sieve ($105 \mu\text{m}$ apertures), and this charge in turn was passed through a No. 325 sieve ($44 \mu\text{m}$ apertures). The powder remaining on the latter sieve consisted of single-crystal Si particles in the size range $44\text{-}105 \mu\text{m}$; although smaller particles would have permitted preparation of a more uniform sample for x-ray purposes, the sieved powder was adequate.

Masking tape was used as a "floor" in the sample aperture of a standard diffractometer sample holder, the tape was sprayed with Krylon, and layers of dispersed powder and Krylon were built up to form the reference sample. After drying, the sample was used to produce reference diffraction lines free of particle-size broadening.

The width of an x-ray diffraction line is usually measured as the breadth at half-maximum intensity and is expressed as an angular width, in terms of the Bragg angle. The measured breadth of a Si line exhibiting broadening due to particle-size effects is corrected for the observed zero-broadening breadth of the same Si diffraction line obtained with the reference powder sample, and the resulting value for the broadening is then used in the Scherrer formula to obtain an estimate of the particle (or grain) size.

This method has been applied in the evaluation of grain size in several CVD Si films grown on various substrates to date. For example, two films deposited on single-crystal (01 $\bar{1}$ 2)-oriented sapphire substrates in the course of examination of growth rate uniformity (Section 2.3.3) were evaluated for crystal structure and average grain size. These films were grown in H_2 carrier gas (flow rate 4 lpm) at temperatures of ~ 600 and $\sim 850^\circ\text{C}$, at growth rates of approximately 0.02 and $0.5 \mu\text{m}/\text{min}$, respectively, to thicknesses of ~ 3.5 and $\sim 2.6 \mu\text{m}$, respectively.

They were found by x-ray diffraction examination to be polycrystalline, with average grain sizes of approximately $0.02 \mu\text{m}$ (200\AA) and $0.07 \mu\text{m}$ (700\AA), respectively. In both cases the Si deposition was preceded by a 1250°C etch in H_2 for 15 min. The fine-grained character of the films was not unexpected and is consistent with anticipated variations in Si growth habit as a function of deposition temperature.

It is also consistent with reflection electron diffraction (RED) results obtained with the same films and with the appearance of the Debye rings in back-reflection Laue patterns obtained for the same samples. The latter method - that of examining the "graininess" or continuity of Debye rings in back-reflection patterns - provides a relatively rapid screening procedure for estimating grain sizes in the range down to a few microns.

The line-broadening method has also been applied to determination of average grain size in substrate materials, but the samples examined by this means so far have had grain sizes sufficiently large that no line broadening has been observed.

Attempts were continued to locate a source of polycrystalline Si particle-size samples for providing experimental calibration of line-broadening measurements. No such source has been located, making it necessary to consider preparation of such samples as part of this contract work. However, sized powder preparation in the size range of interest ($\leq 0.1 \mu\text{m}$) requires special techniques and particle-separator apparatus not readily available. Consequently, this will not be pursued further at the present time; line-breadth observations combined with theoretical considerations will be used for the needed x-ray grain size determinations.

A Philips Model 3181S Angle Mode Programmer System, with teletypewriter output, has recently been delivered for use with the x-ray diffractometer system employed in these studies. This equipment will be used for rapid acquisition (with printout) of diffraction line profile data by automatic angle-stepping, counting, and repeat cycling. This will facilitate examination of film samples where line broadening due to grain size is to be measured.

2.5.3 X-Ray Diffraction Determination of Preferred Orientation

The degree of preferred orientation in some of the Si films prepared in these studies has been evaluated by examination of the relative intensities of the principal low-index diffraction lines in the x-ray spectrum obtained with the diffractometer.

For example, in one of the first applications of the technique early in the quarter, a film grown on a single-crystal (01 $\bar{1}$ 2)-oriented sapphire substrate in H₂ (flow rate 4 lpm) at $\sim 1025^\circ\text{C}$ at a growth rate of $\sim 0.5 \mu\text{m}/\text{min}$ to a thickness of $\sim 10 \mu\text{m}$ (but without the pre-deposition high-temperature etch) was evaluated. It and the two films grown at lower temperatures (~ 600 and $\sim 850^\circ\text{C}$) and mentioned in the preceding section were examined for preferred orientation using Cu K-alpha radiation at 50 Kv and 20 ma. Epitaxial growth was found, as expected, in the 1025°C sample, with the (400)Si plane grown parallel to the (01 $\bar{1}$ 2) plane of sapphire - i. e., the surface plane. (This is a previously observed and reported epitaxial relationship.)

With both the ASTM Index line intensities and the intensities from a standard Si specimen as the comparison basis, it was found that the 600°C film was randomly oriented polycrystalline Si, with the very small grain sizes indicated previously. The 850°C film, on the other hand, exhibited a $\langle 110 \rangle$ preferred orientation in the growth direction (i. e., normal to the interface); the {110} planes tended to be parallel to the substrate surface. As noted in Section 2.5.2, this sample had an average grain size several times larger than the low-temperature film but still quite small.

As discussed in Section 2.3.5.2, this procedure has also been applied to the evaluation of substrate materials having polycrystalline structure, such as the fired aluminas. It is expected that the polycrystalline substrate materials that appear to be of major interest - including the glass-ceramics in which firing has produced varying amounts of crystallization and preferential orientation - will be systematically examined by this method prior to carrying out extensive CVD experiments.

Also, careful investigation of the effects of deposition parameters - notably, temperature, growth rate, and doping species and concentrations - on the relative amounts of preferential orientation in the films in the principal low-index directions will be made in order to select the parameters most conducive to controlled columnar-type growth of the Si sheet material.

2.5.4 RED and SEM Analyses

The transmission electron microscope (AEI Model EM6) used on this contract can be operated in the reflection electron diffraction (RED) mode to produce a diffraction pattern of the sample surface, from which the degree of polycrystallinity or crystal perfection can be deduced. Electrons of 100 Kev energy are directed at the sample at a glancing angle (typically $1/2$ to 1°), producing a diffraction pattern characteristic of the crystal perfection. Because of the glancing angle, the effective penetration depth which gives the diffraction pattern is only a few hundred angstroms.

Several CVD Si films produced to date have been examined by this method, used in conjunction with SEM analyses. Because RED samples only the surface region of a film it is often useful to combine the technique with x-ray diffraction studies as well, since the latter methods sample greater thicknesses; the combined evaluation sometimes permits differentiation of surface and bulk structural characteristics in thin-film samples.

A group of Si films grown in H_2 (flow rate 4 ℓ /pm) on single-crystal (01 $\bar{1}2$)-oriented sapphire substrates was evaluated by RED and SEM techniques, both as grown and after two types of chemical etching. The samples were grown at ~ 1025 , ~ 850 , and $\sim 600^\circ C$ at rates of ~ 2 , ~ 0.8 , and ~ 0.01 μ m/min, respectively; final thicknesses were approximately 10, 3.8, and 0.5 μ m. The high-temperature etch in H_2 was not used on the substrates prior to deposition of these films.

The $1025^\circ C$ sample was shown to be single-crystal (100)Si, as expected. The diffraction pattern had sharply-defined Kikuchi bands, indicative of a high-perfection single crystal with a relatively flat surface. The $600^\circ C$ sample gave a weak pattern with extremely faint, broad diffraction rings, indicative of a film containing at best a small amount of extremely fine-grained polycrystalline material.

When viewed with the SEM, the $600^\circ C$ sample surface was smooth and featureless at all magnifications. The $1025^\circ C$ sample appeared smooth upon visual and low-power examination, but at magnifications above 1000X a number of growth defects were visible. These defects are twinned and multiply-twinned regions, commonly found in epitaxial Si films grown on both single-crystal sapphire and bulk Si substrates. As grown, the defects appeared as slight depressions with threefold symmetry.

The 850°C sample had a matte black finish visible to the naked eye, suggesting an anomalous growth pattern. SEM examination revealed large whiskers and irregular growth protruding from the surface, confirming that it was indeed an anomalous sample, contaminated during growth.

Two different types of etchants were used on these samples to delineate grain boundaries and other defects. The first was a modified Sirtl etch, commonly used to delineate growth defects in bulk Si -- a 5:2:1 mixture of H₂O, HF, and CrO₃. Etching for 15 sec clearly delineated the growth defects in the 1025°C film, etching a deep groove between the defects and the surrounding single-crystal region. SEM examination produced striking evidence of the etching, and could have been used to determine quantitatively the defect concentration. Etching of the 600°C film did not change the surface morphology appreciably. The surface remained nearly featureless up to 24,000X magnification with the SEM.

The second etchant used on the 600°C Si-on-sapphire film was KOH:alcohol, the highly anisotropic etchant mentioned earlier. Since the predominant Si orientation on this sapphire orientation is {100} when epitaxy occurs, it was thought this etchant might delineate individual grains by attacking the {100}-oriented planes, even though the film was largely randomly oriented. SEM examination at magnifications up to 25,000X showed that the flat surface of the film remained essentially unchanged in appearance until the entire thin Si layer had been removed, after about 30 sec of etching.

This type of SEM (and occasionally RED) analysis of Si sheet material will be used regularly to evaluate film surface topography, internal crystal structure (including grain size) of the Si films, and characteristics of the film-substrate interfacial region.

Other operational modes of the scanning electron microscope -- including electron channeling pattern generation for characterizing crystal perfection and orientation when grain sizes become sufficiently large, and the electron-beam-induced current (EBIC) mode for observing electrical characteristics such as minority carrier diffusion lengths when potential barriers are introduced--will be employed for sample evaluation as the program develops.

2.5.5 Electrical Measurements

Most of the film evaluation procedures used in the first quarter of the program have related to the delineation of surface and internal structural characteristics. The films have been undoped; no systematic control of the electrical properties of the Si sheet material by impurity doping during or after growth has yet been undertaken.

Consequently, electrical measurements have played only a minor role in the contract work to date. This will soon change, however, as increasing numbers of Si sheet samples are prepared with appropriate doping concentrations on various substrates, both for development of suitable CVD parameters for achieving the necessary properties for efficient photovoltaic action and for actual processing into solar cell structures at OCLI.

As indicated in Section 2.3.6, several attempts have been made to determine the background impurity doping level characteristic of the present CVD reactor system and the reactant gases now in used, by means of measurement of the net carrier concentration in films on sapphire and on high-resistivity single-crystal Si substrates. Both the van der Pauw (Ref 8) and the conventional bridge method have been used to measure the Hall constant and thus the carrier concentration. Figure 2-27 shows one of the CVD films (in this case on single-crystal sapphire) photolithographically etched to produce a Hall-effect bridge pattern. The film in this case was $\sim 3.4 \mu\text{m}$ thick; there are several mask sizes available with this particular pattern, but the one shown is approximately 0.3 cm on a side.

An alternate method of producing the Hall bridge pattern has been evaluated in preliminary experiments with polycrystalline CVD Si films. This method involves the use of the focused beam of a 5 Kw YAG laser Q-switched at 1200 pps and computer-programmed to trace the outline of a bridge pattern in the film. The beam is used either to melt a patterned groove in a protective mask, to be followed by chemical etching in the groove to isolate the bridge, or to melt/vaporize a groove in the Si film directly, in this same pattern. Further work with the technique is in progress.

The hole concentration of $1-2 \times 10^{15} \text{cm}^{-3}$ found in the undoped CVD Si films measured to date is surprisingly high, and indicates some source of acceptor imperfection -- either chemical impurity or physical defect -- that must be identified and minimized. More attention will be given to this problem after the reactor system modifications are completed early in the second quarter.

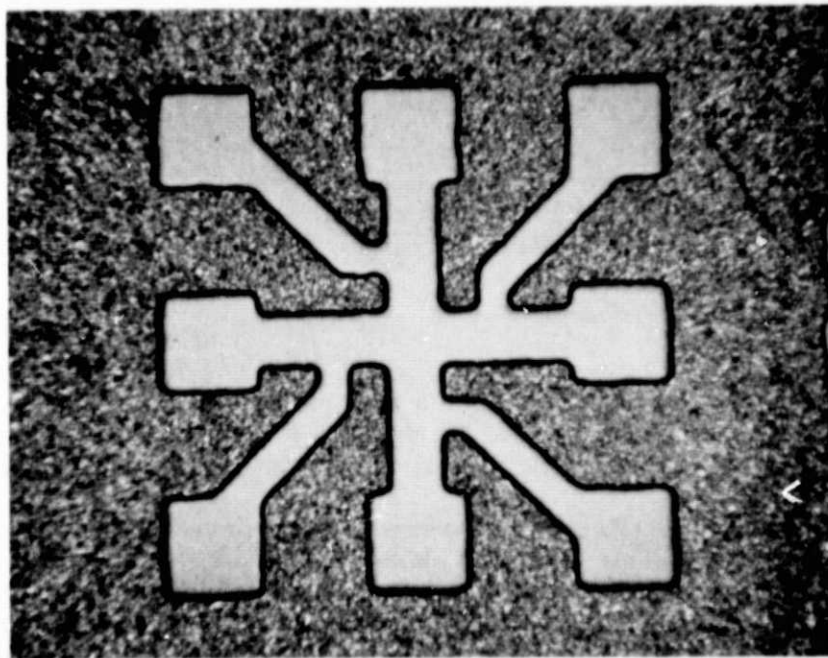


Figure 2-27. Hall-Effect Bridge Pattern Photolithographically Etched in CVD Si Film on Single-Crystal Sapphire Substrate. (Width of current path $310 \mu\text{m}$, length $910 \mu\text{m}$, pattern approximately 2.8 mm square.)

The pulsed MOS C-V method for measurement of minority-carrier lifetimes in Si, which has been applied successfully to the determination of lifetimes in Si-on-sapphire epitaxial material (Refs 9, 10), provides a possible method for determination of this parameter in the polycrystalline films being prepared in this program. The C-V method is also useful for measuring the doping profile vs depth in thin samples. The technique is based on the depletion approximation, and utilizes the capacitance of a capacitor biased in the depletion condition to obtain plots of $\frac{1}{C^2}$ vs V. The slopes of these curves are expected to be proportional to the impurity concentration at the edge of the space-charge layer. However, this technique is limited by the inversion phenomenon.

The pulsed MOS C-V method, in which a short-duration voltage pulse is used to replace the steady dc reverse bias, was introduced as a means to measure the doping profile over a large distance into the Si region. As the technology of MOS devices progressed, it became much simpler and more convenient to study the pulse effect by monitoring the capacitance of an MOS capacitor as a function of time. Using this technique, it was shown that the bulk generation lifetime could be obtained. Zerbst (Ref 11) developed a technique which allowed both the generation lifetime and the surface generation velocity to be extracted from the capacitance-time decay curve.

A schematic diagram of the apparatus used for C-V measurements is shown in Figure 2-28. For the C-t measurements the x-y recorder is simply replaced by a storage oscilloscope. Preliminary attempts to obtain a lifetime value for an undoped CVD Si film grown in H₂ at ~1025°C to a thickness of about 3 μm were unsuccessful,

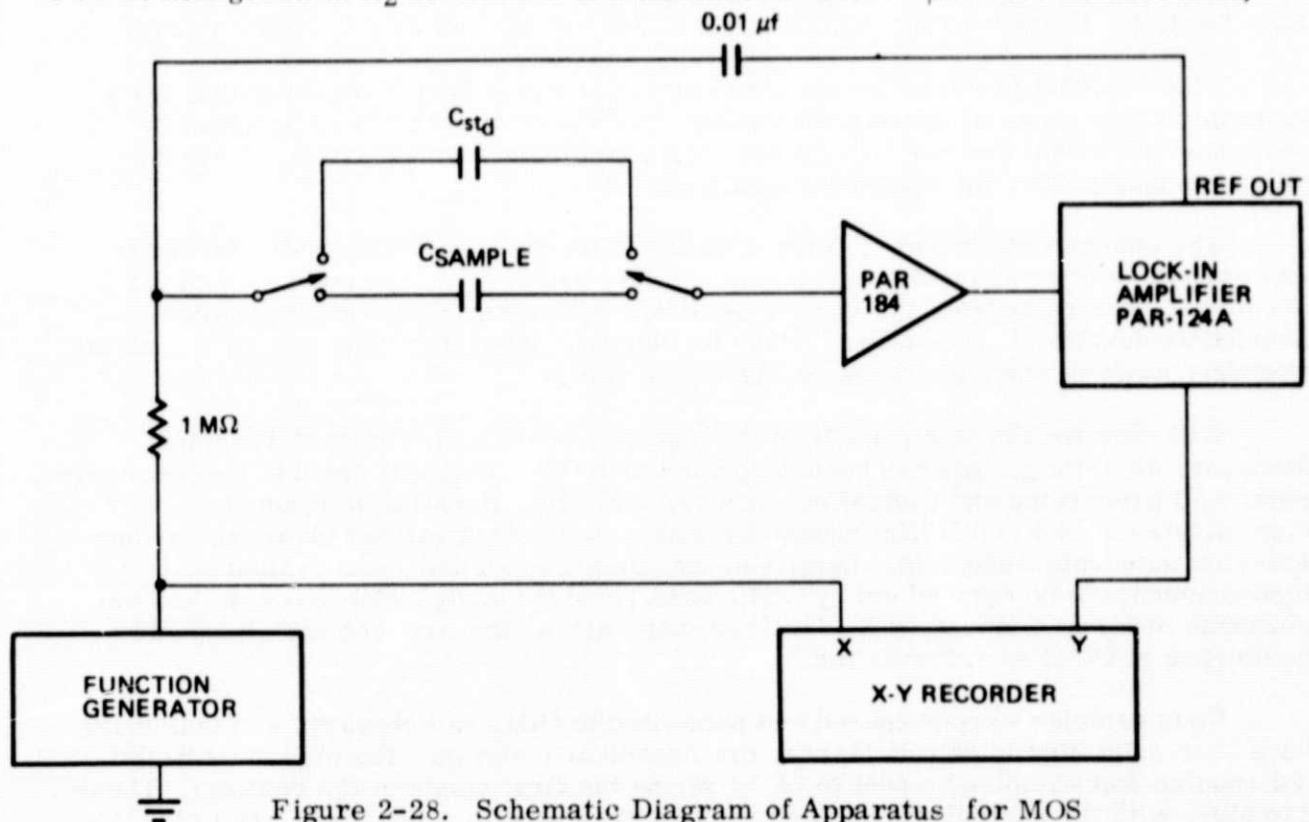


Figure 2-28. Schematic Diagram of Apparatus for MOS Capacitance-Voltage Measurements

but work with the method on this and other similar samples is continuing. As indicated earlier, other methods for determination of effective minority carrier diffusion lengths -- such as the EBIC mode of operation of the SEM -- are also under consideration, and may prove more practical for the polycrystalline films involved in this work.

A preliminary evaluation of the feasibility of using spreading resistance measurements for evaluation of the electrical properties of the polycrystalline CVD Si films has been initiated. The highly specialized apparatus used for spreading resistance measurements is not available at Rockwell at the present time, but a specialty laboratory - Solecon Laboratories - that works exclusively with this analytical method is located in Costa Mesa, CA, only a short distance from the Rockwell facility in Anaheim. Rapid-response service by this experienced and highly-qualified laboratory is available, so excellent analytical assistance is readily accessible.

The major question to be answered is the validity of this type of measurement on polycrystalline Si material having grain sizes and other properties such as those anticipated for the samples to be produced on this contract. A resistivity limitation of $10^3 - 10^4$ ohm-cm characterizes the method and the apparatus now in use; films with effective resistivities less than that should be susceptible to spreading resistance analysis, with good spatial resolution. Several exploratory measurements on representative samples are now being made to determine the utility of the method for this work.

2.6 TASK 6. FABRICATION AND EVALUATION OF SOLAR CELL STRUCTURES

This contract provides for the fabrication and evaluation of experimental solar cells in CVD Si sheet on various substrates. This part of the work is provided by personnel of Optical Coating Laboratory, Inc., Photoelectronics Group, in nearby City of Industry, CA, on a purchased-services basis.

The contract Statement of Work stipulates that the contractor shall "fabricate and evaluate solar cells with a minimum of 1 cm^2 area . . ." and that "techniques for producing solar cells from these films shall be, to the maximum extent possible, previously developed procedures." It is further stipulated that "one solar cell, on the average, shall be made per week during this program."

With this requirement, and with the approval of the JPL Contract Technical Manager, an arrangement has been developed with OCLI that will provide the necessary solar cell processing and evaluation work yet still allow Rockwell personnel to concentrate on the Si CVD film nucleation and growth investigations involving various low-cost substrate materials. Details of the sample processing and evaluation measurements to be carried out by OCLI were resolved early in the quarter, and the purchase order was issued by Rockwell so that work on the contract samples could commence at OCLI soon thereafter.

Four samples were prepared and submitted to OCLI in February, and four more have been submitted to date in March; the Technical Program Plan (Appendix B) did not require that samples be sent to OCLI during the first month of the contract. These samples, with the pertinent deposition parameters and film properties, are listed in Table 2-11.

Table 2-11. CVD Si Sheet Samples* Submitted to OCLI for Solar Cell Processing and Measurement

Sample Desig. and (Month)	Substrate and (Thickness)	Observed Depos. Temp. (°C)	Carrier Gas and (Flow Rate)	SiH ₄ Flow Rate (ccpm)	Film Thickness (μm)	Average Growth Rate (μm/min)	Sample Dimensions (cm) (Approximate Area in cm ²)	Film Structure and/or Surface Texture
OCLI-1 (2/76)	(011̄2) Al ₂ O ₃ [†] (500 μm)	605	H ₂ (4 lpm)	10	3.5	-0.02	r=1.9** (3.6)	Poly; Random Orientation
OCLI-2 (2/76)	(011̄2) Al ₂ O ₃ [†] (500 μm)	860	H ₂ (4 lpm)	10	2.6	-0.5	r=1.9** (3.0)	Poly; Preferred (110) Oriented
OCLI-3 (2/76)	(011̄2) Al ₂ O ₃ [†] (500 μm)	1032	H ₂ (4 lpm)	5	3.0	-2.0	r=1.9** (2.5)	Epitaxial
OCLI-4 (2/76)	Multicrystalline Al ₂ O ₃ [†] (525 μm)	1025	H ₂ (4 lpm)	10	8.6	-1.7	2.2 x 1.9 (oval) (3.3)	Epitaxial in Separate Grains
OCLI-5 (3/76)	(011̄2) Al ₂ O ₃ [†] (500 μm)	1030	H ₂ (4 lpm)	5	10	-2.0	r=1.8** (2.5)	Epitaxial
OCLI-6 (3/76)	ASM805 Alumina (~640 μm)	1025	H ₂ (4 lpm)	25	20	-3.3	1.5 x 2.0 (3.0)	Poly; Preferred (110) Oriented; Directionally Reflective
OCLI-7 (3/76)	ASM805 Alumina (~640 μm)	1021	H ₂ (4 lpm)	10	24	-1.6	1.4 x 1.9 (2.7)	Poly; Preferred (110) Oriented; Directionally Reflective
OCLI-8 (3/76)	ASM805 Alumina (~640 μm)	1030	H ₂ (4 lpm)	25	40	-3.3	1.8 x 1.6 (2.9)	Poly; Preferred (110) Oriented; Directionally Reflective

* All Si films undoped.

† These substrates not subjected to high temperature H₂ etch before deposition.

** These samples approximately 90 deg sector of circle of radius r cm.

Three of the first four Si films were deposited on single-crystal (01 $\bar{1}$ 2)-oriented sapphire substrates that were 500 μm thick, as used in the CVD parameter investigation discussed earlier (Section 2.3). The fourth film was deposited on a multi-crystalline sapphire substrate containing numerous large and elongated individual grains, with some of the grain-boundary intersections with the polished surface being nearly parallel. No attempt was made to establish the crystallographic orientations of the individual grains, although the 525- μm -thick wafer was cut with a nominal (01 $\bar{1}$ 2) orientation. This substrate provided a Si film with numerous relatively large single-crystal regions and numerous grain boundaries, to present a film of intermediate difficulty for the standard solar cell processing to be undertaken by OCLI.

The fifth sample sent to OCLI for solar cell processing and evaluation was another undoped epitaxial Si film grown on (01 $\bar{1}$ 2)-oriented sapphire in H_2 at $\sim 1025^\circ\text{C}$. This sample is to be used for double diffusion processing to produce a photovoltaic junction. The other three samples consisted of sizeable pieces of thick Si films grown on ASM805 alumina substrates in H_2 at $\sim 1025^\circ\text{C}$, at two different growth rates to thicknesses of about 20 and 40 μm , and previously described in Section 2.3.5.2.

Although details of the handling, processing, and measurement techniques applied to any one sample at OCLI will be varied to accommodate the characteristics and/or limitations of the sample, there is a projected sequence of activities that will generally be followed to whatever extent possible. Thus, standard and near-conventional solar cell processing methods will be used, to allow correlation of results with those obtained with conventional bulk single-crystal Si cells. If such procedures exhibit limiting deficiencies when applied to the Si sheet material, then the procedures will be modified and/or novel processing methods must be devised. It is intended that sufficiently rapid feedback of results will occur to permit timely influence of these results on subsequent CVD experiments at Rockwell.

The Si sheet samples received by OCLI will first be routinely checked for thickness, conductivity type, and resistivity, by standard methods. In some cases a preferential etch will be applied to delineate individual crystallites in selected areas, and various surface treatments will be used, if necessary, to prepare the sample for p-n junction formation. A small region of the sample will be tested to determine if Schottky barriers of sufficiently good characteristics can be formed on the sheet surface to permit measurement of the minority carrier diffusion length in the as-received material; if found feasible, such measurements will be made.

A junction will be formed by diffusion of phosphorus or boron, depending upon the conductivity type of the sheet sample. (In those cases where conventional diffusion temperatures are too high for the sample involved, other barrier formation methods -- such as ion implantation -- may have to be introduced.) Diffusion oxides will be removed and open-structure ohmic contacts will be applied, using conventional deposition methods. The junctions will then be isolated to reduce edge-leakage, and in some cases antireflection coatings will be applied to permit more accurate measurement of conversion efficiency.

Because of the nature of the Si sheet samples it may be that conventional processing techniques can not be successfully applied. Thus, the presence of excessive numbers of grain boundaries, a high concentration of carrier lifetime "killer" impurities, uneven sheet surface morphology, irregular or specially-shaped cell configurations, temperature limitations associated with various substrate materials, and special contact configurations necessitated by the use of insulating substrate materials for the Si sheet growth may require development of alternative processing methods. It is expected that these will be established at the time, to meet the needs of the specific situation.

With illumination from a defined light source, such as the AM1 spectrum from a solar simulator, the conventional photovoltaic parameters I_{sc} , V_{oc} , P_{max} , CFF, and power conversion efficiency will be determined. The diffusion length of minority carriers in the completed cell structure will be determined, if possible, by a photovoltaic method using a monochromatic light source. For samples in which the uniformity of photoresponse is of interest (for example, to examine effects of grain boundaries) a photocurrent scan of the surface of the sheet will be made using a small-diameter (10 μm) light spot to compare the output of various regions of the sample.

An array of small-diameter mesa diodes will be formed on the junction structure by etching techniques. These diodes will be evaluated separately to indicate the degree of homogeneity in the sample and correlate the electrical properties with any visible structural features (e. g., grain boundaries). Diode measurements will include the photovoltaic parameters I_{sc} and V_{oc} , the dark forward diode characteristic, junction capacitance, and possibly an evaluation of trap properties.

Complete reports of all data and related observations concerning the sheet samples will be supplied to Rockwell by OCLI. Technical consultation on the correlations between observed sheet properties and the details of the CVD sheet growth process will take place regularly as part of the working arrangement.

At the time of preparation of this report results on the first four samples were not complete, and work had not commenced on the four samples submitted in March. Preliminary results on the first group, however, indicated that considerable difficulty had been encountered in processing the samples because they were quite thin ($\sim 3 \mu\text{m}$, except for OCLI-4) and were undoped. Both OCLI-3 and -4 were found to be slightly n-type, whereas OCLI-1 and -2 had such high resistivity that they did not permit conductivity-type detection even with a very sensitive probe.

On the strength of that evidence, however, all four samples were boron-diffused to attempt to form a p-n junction. Mesas of various sizes were formed by etching, but no evidence of any rectification or photovoltage was found in any one of the samples.

Further work is in progress on these samples, but it appears that the main benefit to be realized from the first group of samples is considerable experience in handling and processing samples that are decidedly non-standard to the solar cell industry. This result is not at all unexpected.

Results on the more recently submitted samples, plus further information on the first group of four, will be given in subsequent reports.

3. CONCLUSIONS AND RECOMMENDATIONS

With all needed components and instruments now received, the modification of the CVD reactor system can proceed and should be completed early in the second quarter. This will require that the reactor be unavailable for CVD experiments for about two weeks, after which exploratory depositions will be resumed in the system, with improved control, reliability, and versatility. The efficiency of the entire procedure of preparing films using specified CVD parameters will be greatly improved.

The response of most of the glass and ceramic manufacturers contacted for assistance in solving the substrate problem has been excellent. Both commercially-available and specially-prepared materials have been supplied for evaluation as potential low-cost substrates. Although the results obtained to date with several commercial glasses have not been encouraging, better results are expected for deposition of Si on special glasses capable of withstanding higher temperatures.

The results obtained for CVD Si growth on fired polycrystalline ceramics - especially alumina - have been moderately encouraging. Aluminas with enlarged grains resulting from special supplementary firing procedures appear promising, although all of these materials have a surface topography that is not conducive to smooth Si layer growth by CVD. Differences in the properties of Si films grown on mechanically-polished polycrystalline ceramic substrates and those grown on the as-fired surfaces will be compared.

High-temperature glass-ceramics - which can be given a variety of surface crystal structures and surface roughness by control of the nucleation and devitrification processes - are of considerable interest and will be tested as substrates as soon as representative samples are obtained. Those high-temperature materials that offer reasonable surfaces for Si deposition and growth are especially interesting, particularly if they are stable in H₂ at elevated temperatures.

The observed differences in Si deposition rate by SiH₄ pyrolysis at temperatures above 850-900°C in H₂ and in He tend to discourage the use of He at the higher temperature because of the increased time required to obtain a given Si film thickness. Further, the film thickness uniformity across the pedestal was much better for Si deposited in H₂ than in He, particularly at higher temperatures. Additional experimentation is required to establish properly the characteristics of Si growth by SiH₄ pyrolysis in He, although it appears that H₂ is more satisfactory for use whenever the properties of the substrate material allow it. Substrates unstable in H₂ might be first covered by a Si film grown in He followed by further Si growth in a H₂ atmosphere in order to improve film thickness uniformity and reaction efficiency.

The non-uniform temperature distribution on the 5-cm-diameter pedestal now in use requires some allowance in planning experiments with either a single large substrate or more than one substrate. The required investigations of substrate surface stability, Si film nucleation and growth phenomena, and the structural and electrical properties of Si sheet material grown on various inexpensive substrate materials can be carried out quite adequately with the present deposition chamber configurations and dimensions. However, some attention will be given to improving the uniformity of the temperature distribution on the pedestal.

Film growth studies will be continued according to the Updated Technical Program Plan given in Appendix B. Several planned variants on the straightforward deposition of Si films by SiH_4 pyrolysis will be investigated, to attempt to influence the early stages of growth of the Si films and thus the ultimate properties of the resulting sheet material. The use of HCl in the SiH_4 gas stream, to attack smaller crystallites and allow larger ones to grow more rapidly, will be examined. Similarly, the use of the two-step deposition process, employing SiH_4 and one of the hydrides, may accomplish the same thing. In situ annealing of partial layers, to enhance grain size before further deposition occurs, and the use of a light deposition (i. e., a partial layer) of a metal on the substrate to produce nucleation sites for the depositing Si and thus enhance growth of larger grains, will also be investigated.

A variety of procedures for evaluating the properties of the substrates as well as the CVD Si sheet material is being developed. It will be increasingly important to be able to correlate substrate properties with film properties, so improvements in speed of sample analysis will be needed. Because of the complex physical structure and the mechanisms of charge transport in the polycrystalline Si films, the nature of the measurements made and the interpretation of the results of these measurements must be given careful consideration. When the properties of the Si films have improved sufficiently, additional evaluation techniques--such as Schottky-barrier methods and spreading resistance measurements for determination of impurity distributions, EBIC-mode analysis with the SEM to investigate properties of individual crystal grains and the intervening grain boundaries, and surface photovoltage measurements to obtain effective minority carrier diffusion length values--will be applied to give more complete and accurate understanding of the Si sheet properties.

The first attempts to apply standard solar cell processing to some of the films prepared to date have indicated that it may become necessary to develop and/or apply some specialized methods - for example, ion implantation doping instead of, or in addition to, diffusion doping for junction formation - to these polycrystalline Si films in order to get an adequate indication of their suitability for solar cell fabrication. It is recommended that this possibility be given consideration in the near future, depending upon further results to be obtained at OCLI with other samples of CVD Si films, even though initial program plans did not place a high priority on such process development.

4. PLANS FOR THE NEXT QUARTER

The planned work for the next quarter will follow the Updated Technical Program Plan given in Appendix B of this report, to the maximum extent possible.

Summarized by task, the planned work is as follows:

Task 1

1. Complete installation of new reactor system components and controls.
2. Test modified reactor system upon completion.
3. Prepare written Standard Operation Procedure for modified reactor system, as required by contract.
4. Conduct Design and Performance Review of reactor system for JPL personnel, as required by contract.

Task 2

1. Continue experimental evaluation of candidate substrate materials by Si CVD experiments as suitable samples become available, and continue/complete screening of materials received during first quarter.
2. Continue interactions with potential suppliers of substrate materials.
3. Compare properties of as-fired and mechanically-polished alumina substrates from several suppliers, and compare Si film properties grown on both types.
4. Continue to investigate the effects of various substrate surface treatments on the resulting Si film properties.

Task 3

1. Continue experiments to identify preferred CVD parameters as well as candidate substrate materials for Si film growth.
2. Continue experiments with two-step deposition process on selected substrate materials.
3. Pursue investigation of effects of doping impurities on Si film growth phenomena and on Si film properties.
4. Initiate study of the effects of in situ and post-growth annealing on final properties of the Si film.

Task 4

1. Prepare additional groups of CVD Si film samples for material characterization studies, as needed.
2. Prepare samples of Si sheet material on various substrates for fabrication of solar cell structures at OCLI.

Task 5

1. Continue to use X-ray line broadening technique for grain-size determination, provided film properties still fall in useful range of the method; employ new angle-mode programmer system for automated acquisition of line-width data.
2. Continue to evaluate preferred orientation in polycrystalline substrates and in Si films by X-ray diffraction techniques, and investigate systematic variations in such orientation with changes in CVD parameters (e.g., deposition temperature).
3. Investigate feasibility of using dark-field transmission and replica electron microscopy methods to determine crystallographic orientation in selected samples.
4. Apply optical microscopy, scanning electron microscopy, and RED techniques to determination of surface topography and structure and internal grain structure of CVD Si films on glasses and ceramics.
5. Initiate study of modeling of polycrystalline Si films on various substrates, for purposes of making proper interpretation of electrical measurements.
6. Evaluate and apply spreading resistance method for obtaining profile of electrical properties (and thus impurity and/or defect concentrations) in polycrystalline Si films.
7. Attempt to measure minority carrier lifetime in CVD Si films on various substrates, using pulsed C-V method in MOS structures.
8. Investigate feasibility of using EBIC mode of SEM for evaluation of minority carrier transport properties in polycrystalline Si films.
9. Undertake comparison of van der Pauw and bridge methods for measurement of charge transport properties in CVD Si films.
10. Continue evaluation of laser etching method of defining Hall bridge patterns in Si film samples.

Task 6

1. Meet with OCLI technical personnel, as needed, to discuss and correlate results obtained on CVD Si samples processed/evaluated to date.
2. Prepare and submit additional samples of CVD Si sheet to OCLI for solar cell processing and evaluation, emphasizing films on fired polycrystalline alumina substrates and other high-temperature materials.

5. NEW TECHNOLOGY

No reportable items of new technology have been identified during the conduct of the first quarter's work on this contract, which is the period covered by this report.

PRECEDING PAGE BLANK NOT FILMED

6. REFERENCES

1. See, e.g., H. M. Manasevit, D. H. Forbes, and I. B. Cadoff, *Trans. Met. Soc. AIME* 236, 275 (1969).
2. E. Rasmanis, at The Electrochemical Society, Spring Meeting, Pittsburgh, April 1963, Paper No. 72.
3. See, e.g., Y. S. Chiang, The Electrochemical Society, Spring Meeting, Chicago, May 1973, Paper No. 119; also, P. Rai-Choudhury and P. L. Hower, *J. Electrochem. Soc.* 120, 1761 (1973).
4. S. Horiuchi, *Solid-State-Electron*, 18, 1111 (1975).
5. T. I. Kamins and T. R. Cass, *Thin Solid Films* 16, 147 (1973).
6. See, e.g., Y. S. Chiang and D. Richman, *Met. Trans.* 2, 743 (1971); also see Ref 7, Section 3.
7. R. P. Ruth, A. J. Hughes, J. L. Kenty, H. M. Manasevit, D. Medellin, A. C. Thorsen, Y. T. Chan, C. R. Viswanathan, and M. A. Ring, "Fundamental Studies of Semiconductor Heteroepitaxy," Final Report, August 1973, APRA Order No. 1585, Contract DAAH01-70-C-1311. (Prepared by Rockwell International, Electronics Group, Research and Technology Division, Anaheim, Ca., for USAMICOM, Redstone Arsenal, AL), p. 96 et seq.
8. L. J. van der Pauw, *Philips Res. Repts.* 13, (1958).
9. D. K. Schroder and P. Rai-Choudhury, *Appl. Phys. Lett.* 22, 455 (1973).
10. Denis J. McGreivy and C. R. Viswanathan, *Appl. Phys. Lett.* 25, 505 (1974).
11. M. Zerbst, *Z. angew. Phys.* 22, 30 (1966).

PRECEDING PAGE BLANK NOT FILLED